April 07, 2015

Project Summary (2012-2015) – Carbon Dynamics of the Greater Everglades Watershed and Implications of Climate Change

Annual Report (2014-2015)

Objective 1. **Quantify above- and belowground carbon stocks of terrestrial ecosystems along a seasonal hydrologic gradient in the headwaters region of the Greater Everglades watershed.**

Some major accomplishments were completed this year with quantifying carbon storage as a result of the geophysical data collection and analyses. Geophysical surveying during Year 3 was focused on completing the work form Year 2 as related to the estimation of belowground carbon stocks at the Disney Wilderness Preserve (DWP) site. As explained below a few additional GPR surveys were conducted to expand those performed during Year 2 and complete a first draft of a journal manuscript based on these results. Additionally, a laboratory study to investigate biogenic gas dynamics from peat monoliths from 3 different sites using hydrogeophysical methods was also completed as explained below.

Following measurements from Year 2 ground penetrating radar (GPR) surveys were performed at several locations within the preserve, including the depression marsh site and several other depression marshes within the footprint of the pine flatwoods site EC site. Although several long common offset profiles were performed at different locations within the preserve (i.e. Figure 1), the main goal was to transect wetland depressions in order to investigate: 1) the extent of organic deposits within the depressions (i.e. carbon content); and 2) whether any lithological controls may exist for the location and lateral extent of these depressions within the preserve.

As related to 1), and following measurements from Year 1 and 2, the main target for surveys related to peat thickness estimation (i.e. carbon stock determination) was to image the interface peat-mineral soil in order to estimate peat thickness at high spatial resolution. Figure 2 shows a 140 m long GPR common offset profile collected along one of the depression marshes shown in Figure 1 with a trace spacing of 0.2 m. The GPR profile depicts a marked basin-like shape reflector corresponding to the interface peat-mineral soil with a maximum peat thickness of 0.9 m as confirmed from direct coring at the center of the basin (Figure 2). During Year 3 a full core was collected within this depression and analyzed for carbon content. Results are also shown in Figure 2 confirming two sharp interfaces with contrasting carbon contents that coincide with the location of sharp reflections in the GPR profile. Since reflections in GPR are based on reflection coefficients as related to contrasts in physical properties of the subsurface (i.e. mineralogy, water content, porosity, etc), it seems reasonable to expect that strong contrasts in carbon content will result in strong reflection coefficients and this marked reflectors.

Figure 2: GPR common offset profile across the first wetland depression shown in Figure 1. Direct coring confirmed the presence of lithological boundaries associated with thickness of the organic soil layer that resulted in marked reflections in the GPR record. Carbon analysis of a full core also confirms these boundaries.

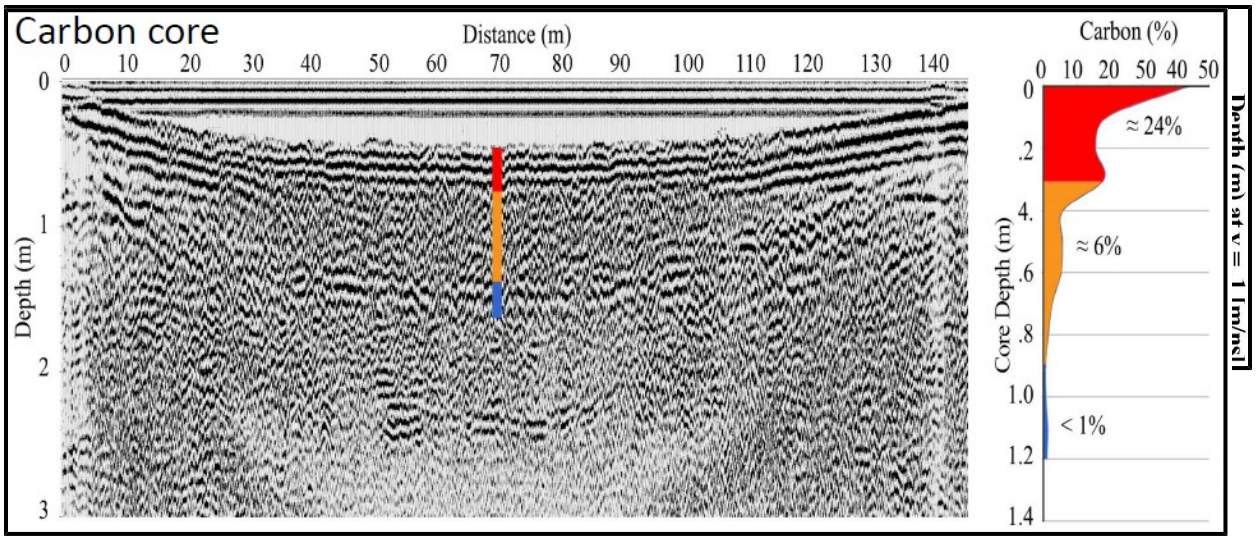

In order to further constrain the geometry of the basin at selected depressional wetlands and following measurements during Year 2, three dimensional (3D) surveys were performed in two different wetlands to investigate peat thickness variability along within the entire depression. The survey consisted of a series of 10 to 20 GPR common offset profiles spaced 5 to10 m (depending on size of the marsh) and extending from one edge to the other of the feature. Figure 3 shows the experimental setup for a 3D GPR survey along the marsh shown in Figure 2. A 3D model of peat thickness for the same depression marsh is also depicted in Figure 4. Based on this model and accounting for C contents as determined from core values in Figure 2, basin volume for the depression is estimated at 9996.88 m^3 of peat or 1,596.5 Mg C.

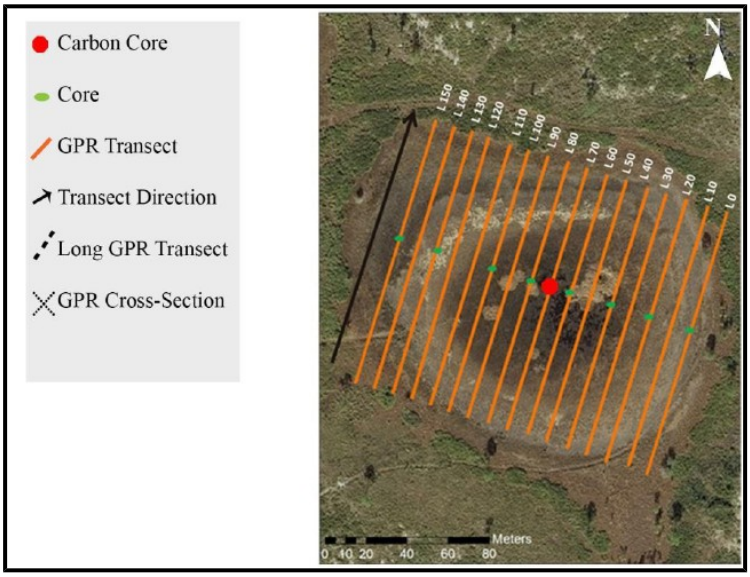

Figure 3: Satellite image of the flatwoods study site showing the location of several depression marshes. Inset shows GPR 3D survey over one of the depression marshes based on 16 GPR common offsets at 10 m spacing.

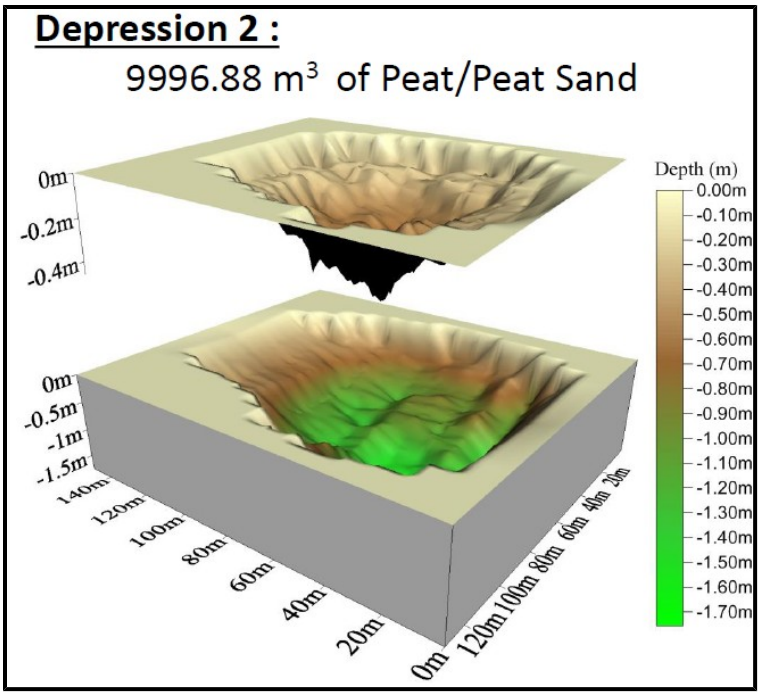

Figure 4: 3D model of peat thickness for the depression marsh depicted in **Figure 2** and **3**.

Based on GPR results and field surveys, a linear relationship between total carbon content (i.e. carbon stocks) and wetland surface area was determined. Using this relationship a carbon stock based on the surface area estimated from the National Wetlands Inventory (Figure 5) was contrasted with field measurements along 5 depressional wetlands and showed good correspondence. The relationship was used to estimate total carbon stock based on the surface area from all depressional wetlands in the preserve and resulted in a total carbon content of 99,537.43 Mg or Mt at 130.4 Kg/m2. These results are consistent with values found in the literature (i.e. 53 -165 kg m−2, Beilman, Vitt et al. 2008) and show the importance of depressional wetlands as an overall contributor of the carbon cycling in the preserve.

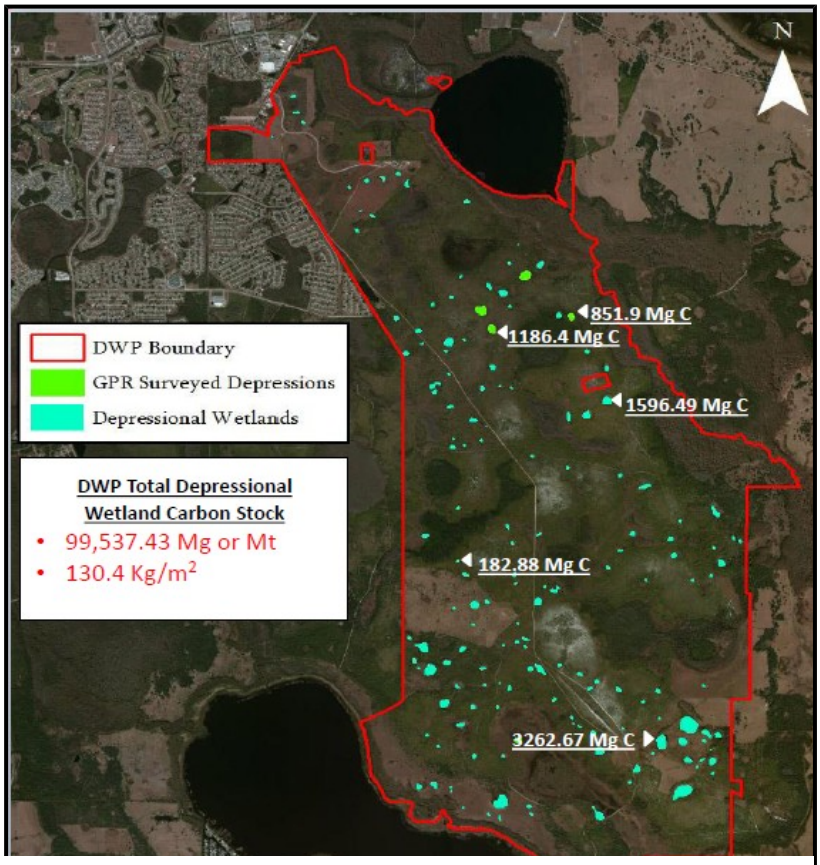

Figure 5: Satellite image showing surface area of depressional wetlands estimated from the National Wetlands Inventory. GPR surveyed depressional wetlands and total estimated Carbon stock based on our modeling are also are indicated.

As related to 2), the potential of lithological controls for the location of depressions was investigated using low frequency GPR antennas. Figure 6 shows a GPR transect using 80 MHz antennas crossing one of the depressional marshes and clearly depicts how subsurface lithology may be dictating the positioning of wetland depressions. A depressional feature can be followed down to depths reaching 35 m. Although more research will be conducted to further confirm correlation with other depressional features, these results indicate that depressional features may originate from subsurface collapses. While depressional features in Florida are often associated to collapses related to dissolution features in limestone it is important to consider that deep cores previously collected at DWP (located about 2 miles from the location of this profile) show sand deposits overlaying clay (interface at 36 m) and a clay-limestone interface at 55 m. If dissolution features in limestone are indeed the origin of these depressional marshes it is remarkable to consider that collapses extent beyond 50 m within the subsurface.

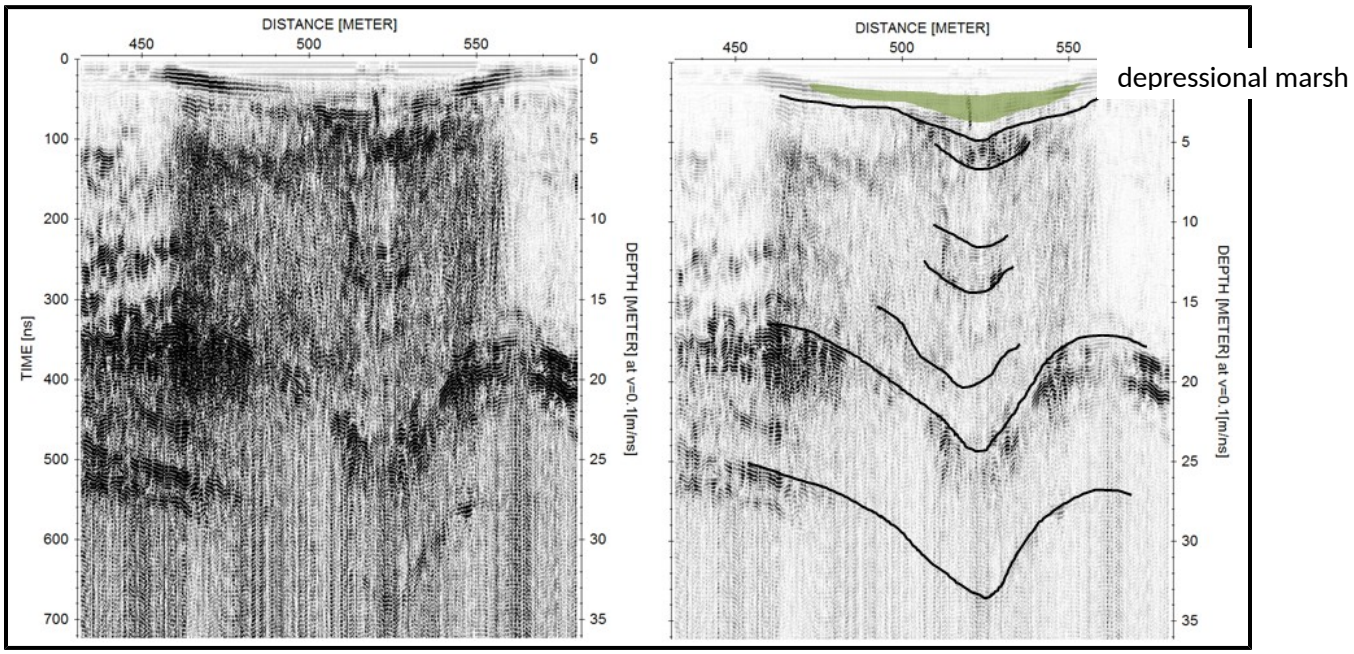

Figure 6: GPR common offset profile (left) and interpreted profile (right) over a depressional marsh using 80 MHz antennas. Interpretation of the reflector record clearly depicts the correspondence between the position of the depressional marsh (indicated in green) and collapse of the subsurface

During year 3, aboveground biomass at Blue Cypress and DWP marsh EC sites was estimated with five 1 m^2 harvest plots from each site, collected in spring and fall 2014. An additional 5 plots will be harvested in Spring 2015. Additionally, decomposition/root ingrowth bags were deployed at all three sites nearby each of the closed gas exchange chambers in August 2014 with a planned 1 year incubation period. Soil

cores were extracted from the decomposition core incubation locations to be used for characterization of soil carbon content.

Future plans related to above- and below-ground harvests and litter/soil chemistry include: 1) analysis of the 50cm deep soil cores from 8 plots per site for characterization of soil properties (bulk density, porosity, volumetric moisture content and gravimetric moisture content), and 2) pulverizing of dried litter and soils for organic:inorganic matter content by loss on ignition and elemental carbon and nitrogen content by elemental combustion analysis.

Objective 2. **Develop budgets of ecosystem gaseous carbon exchange (CO_2 and CH_4) across the seasonal hydrologic gradient at multiple spatial scales.**

We continued flux data collection and analyses at all three sites during year three which included carbon flux measurements (CO_2 and CH_4) at three locations (Pine Flatwoods, DWP Depression Marsh, and Blue Cypress: We upgraded some equipment and installed boardwalks and small chambers at the Blue Cypress marsh.:

1. Added CR1000 and CR850 data-loggers to the Blue Cypress flux station. The new data-loggers will allow continuous monitoring of new parameters related to carbon cycling, such as oxidation-redox potential and barometric pressure.

2. Added a CR10X data-logger to the FAU chamber platform at Blue Cypress. Eight thermistors were wired into the CR10X data-logger to measure water and/or air temperature during carbon flux light-response measurements.

At Blue Cypress we have monitored carbon fluxes over the course of nearly five years in order to determine long-term carbon sequestration rates within a subtropical peat marsh. Some initial results summarized from the Blue Cypress marsh system are shown in Figures 7,8, and 9. During this period we were able to include the impact of fire and water levels on ecosystem carbon cycling in the wetland systems Table 1.

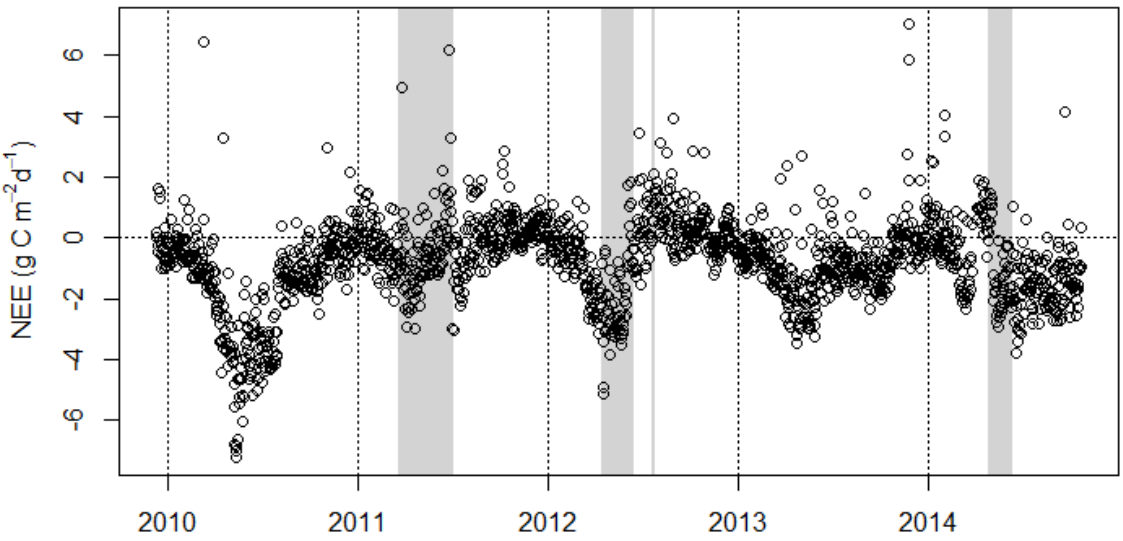

Figure 7: Seasonality and interannual variability of daily net ecosystem exchange over 5 measurement seasons. Shaded areas indicate periods where water level dropped below land surface

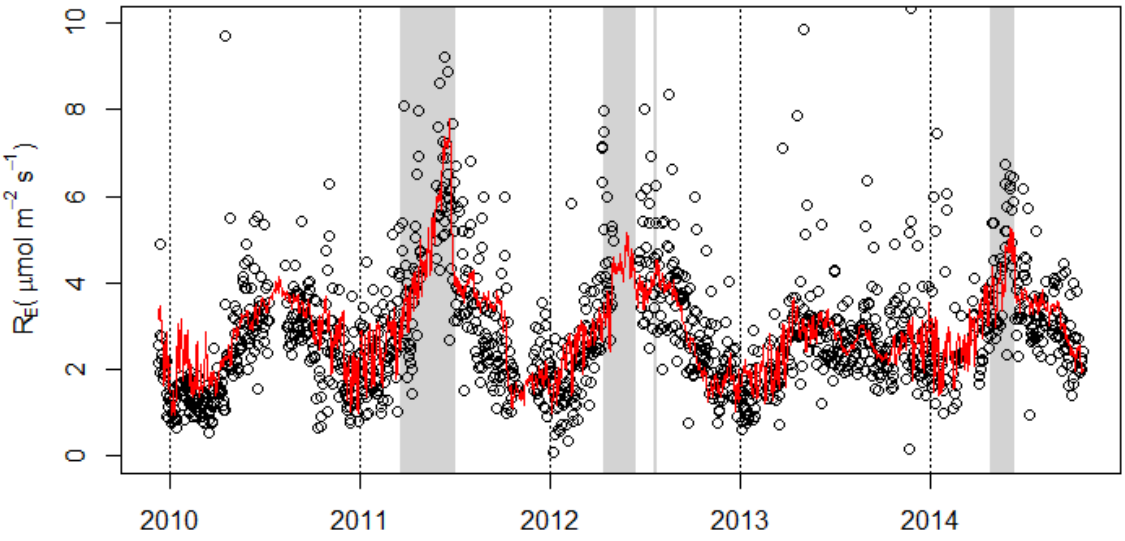

Figure 8: Ecosystem respiration estimated from nighttime NEE. Emperical model fit shown in red

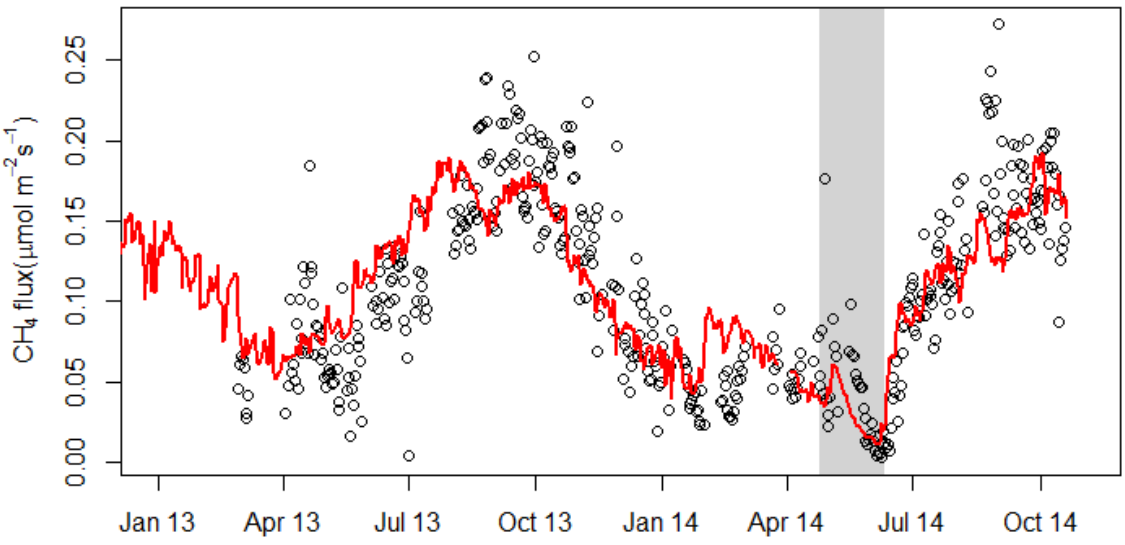

Figure 9**:** Daily average of methane flux since 2013 with. empirical model fit shown in red.

Year	NEP (g C m^{-2})	RE	GEP	CH_4	*wl*<0 (days)
2010	-602	954	1556	33	0
2011	-72	1247	1320	26	104
2012	-136	1183	1319	32	71
2013	-297	977	1274	44	0
2014	-267 (partial)	936	1202	26	40

Table 1**:** Annual sums of net ecosystem productivity, partitioned into assimilatory (GEP) and respiratory (RE) components, methane emissions and length of dry season. Methane fluxes from 2010-2012 are modeled data.

A research paper has been drafted entitled “Fire and water regulate long-term carbon sequestration in a subtropical peat marsh”. The paper summarizes about 5 years of water, energy, and GHG fluxes at the Blue Cypress flux station. Key findings are: (A) Blue Cypress marsh was an annual carbon sink, (B) hydro-period is an important driver of both CO_2 and CH_4 fluxes, as flooding suppresses soil oxidation but enhances anaerobic decomposition of organic matter, (C) post-fire recovery of marsh photosynthetic

capacity occurs within 2-3 months (Figure 10).

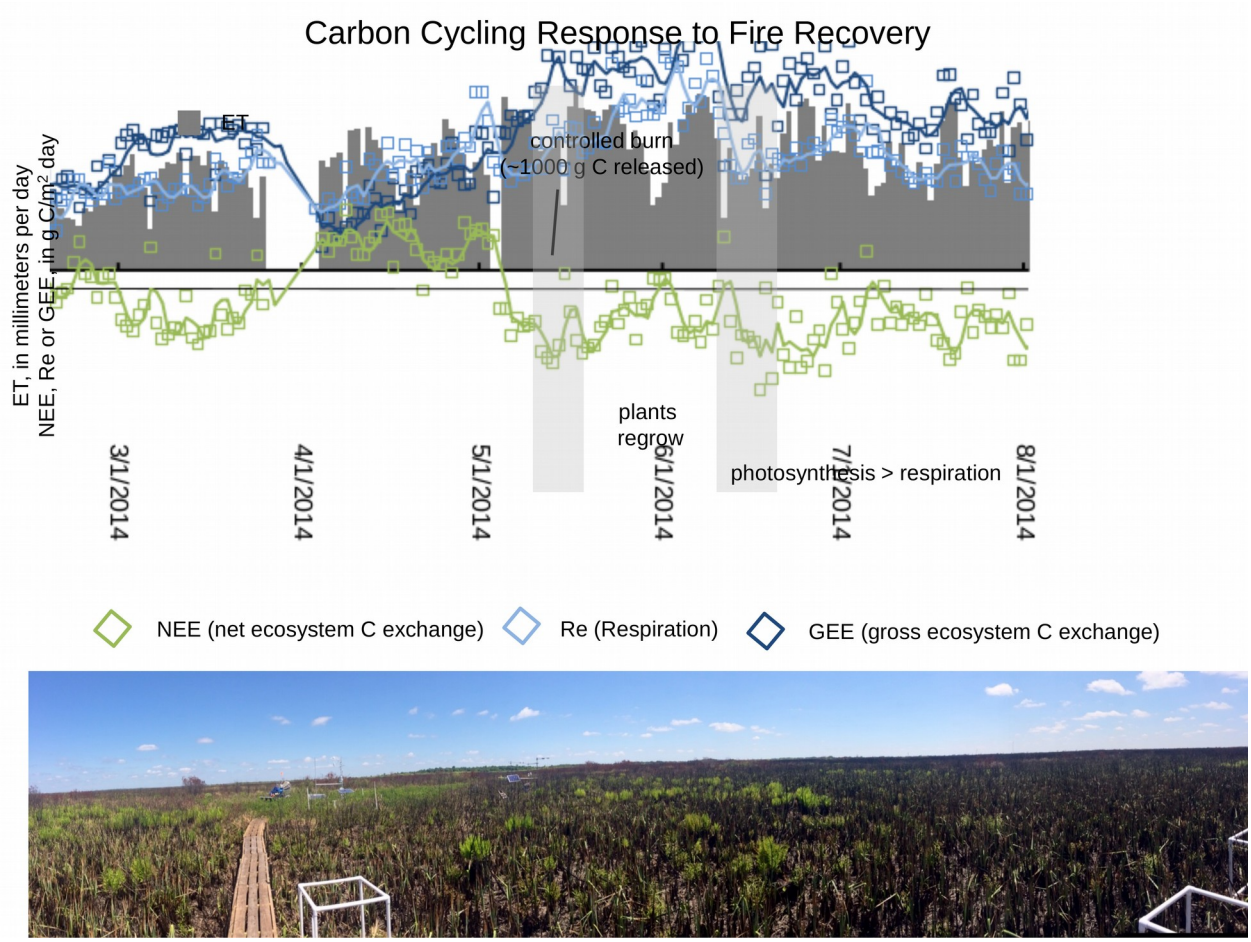

Figure 10. Post fire recovery occurs within 2-3 months. Shows boardwalk for small chamber measurements.

A daily molar methane model was created for gap-filling, as part of the Blue Cypress analyses. The methane model is a power function of continuous variables that explained seasonality in methane emission, specifically, air temperature and flooding. This CH_4 model proved useful in a collaborative study of CH_4 emission over subtropical forested dwarf cypress wetland, as described by Shoemaker et al. (2015, http://www.biogeosciences-discuss.net/11/15753/2014/bgd-11-15753-2014.html).

Chamber measurements of net ecosystem CO_2 exchange continue at all sites (pine flatwoods, EC depression marsh, and Blue Cypress peat marsh; Figure 11). Boardwalks have been installed in the wetlands to prevent disturbance. These measurements will continue in 2015 and open top chambers are being installed on half (4) of the chambers at each site to investigate the impacts of future climate change. Anomalously wet conditions have limited site access to the depression marshes at DWP, but measurements have recommenced both at the EC tower site and an additional small depression marsh

within the pine flatwoods EC tower footprint. Eight chambers are spaced ~10 m apart along a transect radiating from the center of the marsh out to the surrounding palmetto/wiregrass flatwoods. In conjunction with the geophysical surveys (see above), fluxes from these chambers will be used to assess the influence of these small but ubiquitous landforms on landscape carbon exchange.

Assessments of leaf-level water and carbon exchange for the dominant sawgrass (*Cladium jamaiscense*) and willow (*Salix caroliniana*) have been completed at Blue Cypress (Figure 12). In addition to aiding in the model parameterization for photosynthesis and transpiration, this data in conjunction with assessments of species leaf area index, seasonal measurements of PAR and temperature from the EC tower, and vegetation land cover data from the St John's River Water Management District will be used to evaluate the consequences of wetland shrub encroachment on landscape water and carbon cycling. Leaf gas exchange capacity will be assessed from the canopy and/or understory dominants at the remaining sites to aid in model parameterization.

At Blue Cypress, we are also initiating a new experiment (as part of an FAU master's thesis project) to quantify the production, oxidation, and net emission of methane along the soil-water-air continuum. Laboratory incubations will estimate net methane production within the soil and dissolved methane in the water column. Inverted funnels and floating chambers will collect gas released from the soil surface and the water surface, respectively. The existing closed chambers will be used to quantify plant canopy methane emission. Methane emissions will be compared to those monitored by the Blue Cypress eddy covariance tower.

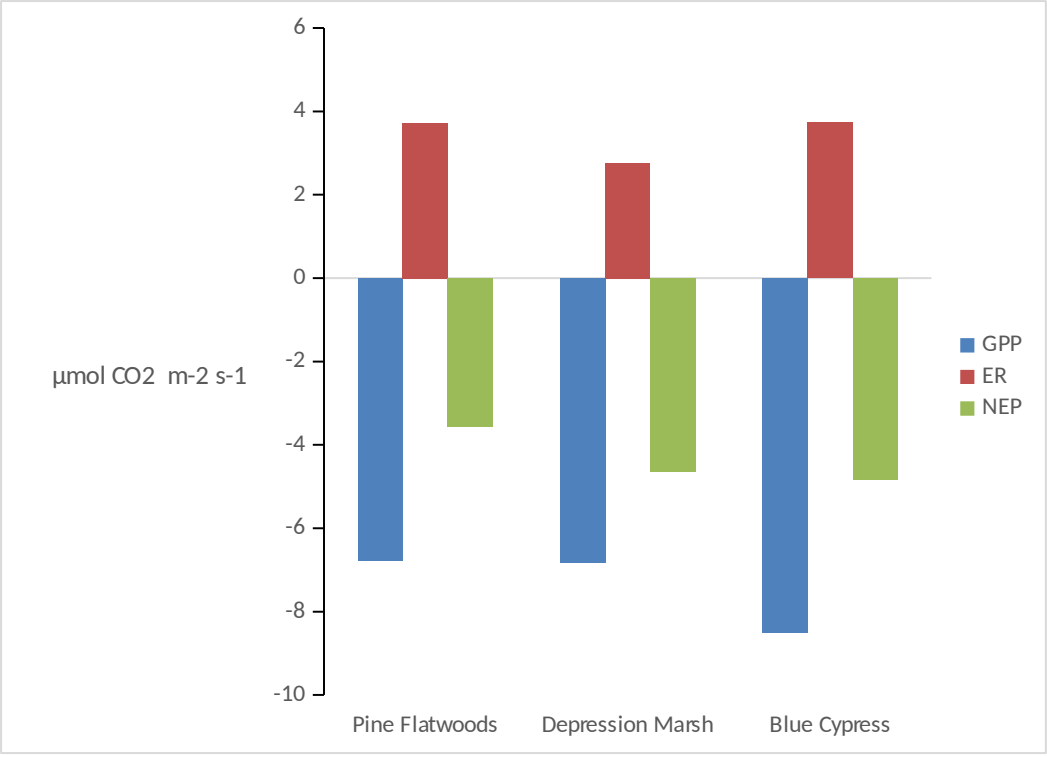

Figure 11. Mean (±S.E.) CO_2 exchange rates from 2013-2015 for each of the three study sites. Negative values indicate uptake of atmospheric CO_2.

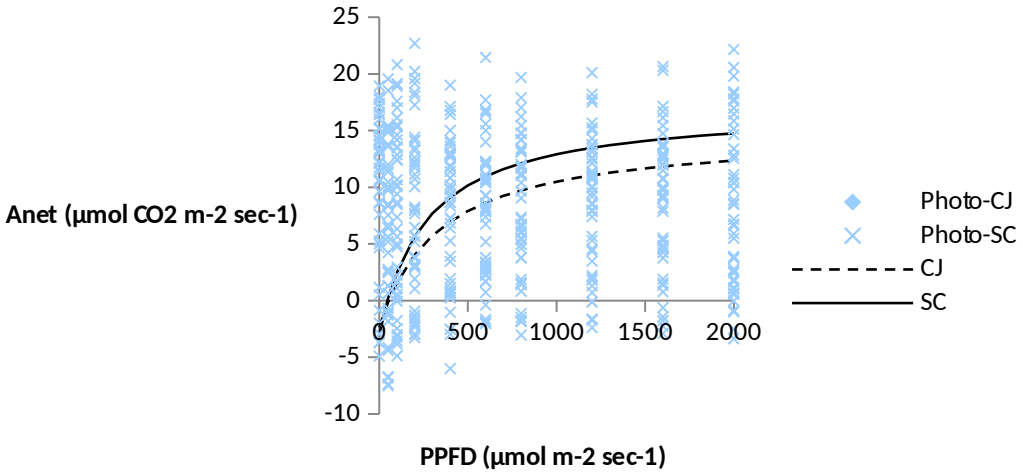

Figure 12. Light response curves for net photosynthetic uptake of CO_2 (A_{net}) of sawgrass (CJ) and willow (SC) at Blue Cypress. Curves represent a rectangular hyperbola model fitted to PPFD-gradient measurements collected from 20 leaves per species.

Geophysical surveying as related to gas dynamics at both DWP and Blue Cypress have been very limited during Year 3 at the field scale. A laboratory experiment however has been conducted to better understand dynamics of gas accumulation and release in 3 peat monoliths from three different ecosystems. The experiment used an array of hydrogeophysical methods (including GPR, time-lapse cameras and gas traps, Figure 13a) to investigate the spatial variability in biogenic gas accumulation and release in three 0.027 m^3 peat monoliths from three different wetland ecosystems (Figure 13b) in central Florida, including a sawgrass peatland, a wet praire, and a depressional wetland within a pine flatwood. High frequency (1.2 GHz) GPR transects were collected along each sample about three times per week and over a period of five months in order to estimate gas content variability (i.e. build-up and release) within the peat matrix. GPR measurements were constrained with an array of gas traps (eight per sample) fitted with time-lapse cameras in order to capture gas releases at 15 minute intervals. Gas collected at the gas traps was analyzed with a gas chromatograph in order to determine CH_4 and CO_2 content. A grid of surface deformation points was also collected concurrently to monitor changes in the peat surface associated with gas build up and release. Figure 13c shows some preliminary results for one of the samples and despite an initial matching between GPR velocity and mass of C as inferred from gas entrapped an inverse relationship seems to exist between the two (i.e. more gas released results in less velocity as indicative of a lower gas content within the peat matrix). Processing of datasets from this experiment is currently ongoing.

Figure 13: a) Experimental setup at the laboratory scale showing GPR and gas trap measurements over a peat monolith; b) full experimental setup showing the three peat monoliths and time-lapse cameras; c) resulting dataset from one the monoliths showing GPR velocities and C mass estimated from gas traps.

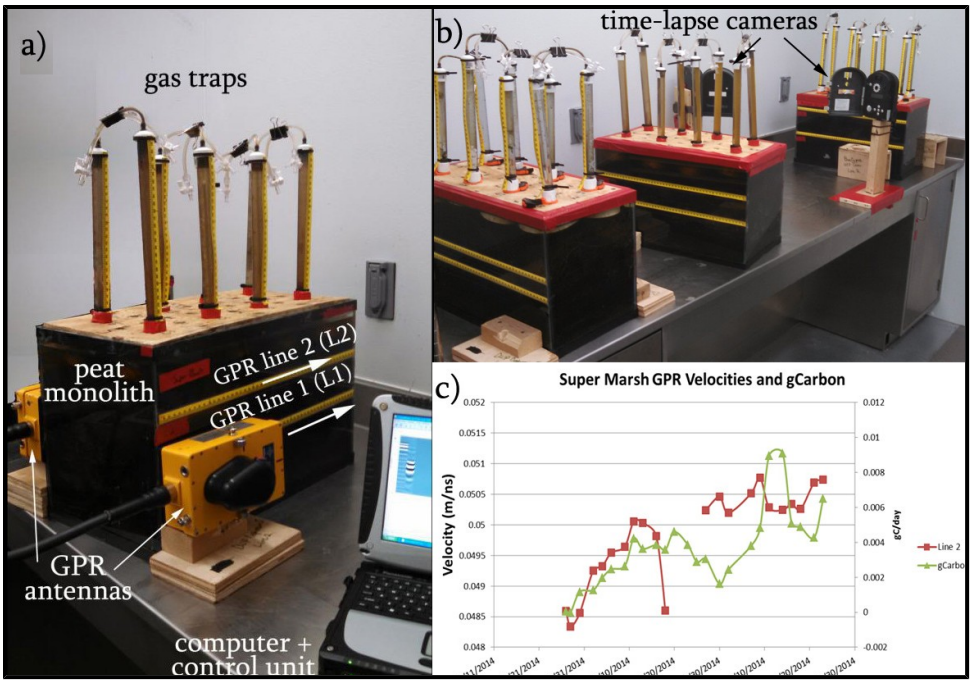

Future work will take a similar approach to the field site. An experiment is currently in preparation to implement a similar experimental design at the field scale and investigate how gas content within the peat matrix evolves over time and results in gas build up and release. The experiment will intend to collect high temporal resolution datasets (i.e. 3-4 measurements a day) for a short period of time (i.e. 7-10 days) and further constrain temporal variability in gas accumulation and release.

Objective 3. **Assess the impact of climate drivers on ecosystem carbon exchange in the Greater Everglades headwater region.**

Passive warming chamber prototypes have been developed and used to finalize the chamber design. Warming treatments will be implemented in 4 of the 8 plots at each of the three sites in April 2015 as well as an additional chamber housing a series of decomposition incubation bags. Wetland soil cores have been collected for a laboratory incubation study to assess the influence of water table position on soil CO_2 and CH_4 emission, to be completed by the end of Summer 2015.

Objective 4. **Integration of research findings from Objectives 1-3 with climate-driven terrestrial ecosystem carbon models to examine the potential influence of projected future climate change on regional carbon cycling.**

Work has been continuing on the development of an Emergent Macrophyte Model (Appendix A, yet to be parametrized) which is being designed to calculate both the uptake of carbon due to growth and the release due to decomposition, in order to calculate the net storage per unit time. In addition, an effort to develop a model for wetlands methane production and carbon storage is highlighted in Appendix B..

Outreach Activities:

Peer-reviewed manuscripts

Published:

Turetsky, MR, BW Benscoter, S Page, G Rein, G van der Werf, A Watts. 2014. Global vulnerability of peatlands to fire and carbon loss. Nature-Geosciences. DOI: 10.1038/NGEO2325

Nungesser, M, C Saunders, C Coronado-Molina, J Obeysekera, J Johnson*, C McVoy, BW Benscoter. 2014. Potential effects of climate change on Florida's Everglades. Environmental Management, DOI: 10.1007/s00267-014-0417-5.

Yang X, Liu C, Fang Y, Hinkle, R., Li, H., Bailey, V., Bond-Lamberty, B... "Simulations of Ecosystem Hydrological Processes Using A Unified Multi-scale Model." *Ecological Modelling*. 2015;296:93-101.

In progress:

McClellan*, M., Comas, X., Benscoter, B., Hinkle, R. Carbon stock estimation in the Disney Wilderness Preserve (Orlando, FL) using hydrogeophysical methods. Manuscript currently in preparation to be submitted to *Journal of Geophysical Research-Biogeosciences*.

Published abstracts

McClellan, M., Comas, X., Wright, W., Mount, G. 2014. Estimating Carbon Stocks Along Depressional Wetlands Using Ground Penetrating Radar (GPR) in the Disney Wilderness Preserve (Orlando, Florida). Abstract B31C-0029 presented at 2014 Fall Meeting, AGU, San Francisco, Calif., 15-19 Dec.

Benscoter, B., McClellan, M., Benavides, V., Harshbarger, D., Comas, X. 2014. Estimating Carbon Stocks and Atmospheric Exchange of Depressional Marshes on the Central Florida Landscape. Abstract B41C-0043 presented at 2014 Fall Meeting, AGU, San Francisco, Calif., 15-19 Dec.

Benscoter, B., Hinkle, R., Comas, X., DeAngelis, D., Shoemaker, B., Sumner, D. 2014. Community Carbon exchange along an ecosystem hydrologic gradient in the Florida Everglades. Joint Aquatic Sciences Meeting 2014, Portland, Oregon. May 18-23.

Other presentations:

McClellan, M., Wright, W., and Comas, X. 2014. Estimating carbon stocks along depressional wetlands using ground penetrating radar (GPR) in the Disney Wilderness Preserve (Orlando, Florida). FAU CES College of Science Graduate Research Day, March 21, 2014. Boca Raton, FL

Graham, SL, DM Sumner, B Shoemaker, BW Benscoter, and R Hinkle. "Water level and fire regulate carbon sequestration in a subtropical peat marsh." American Geophysical Union Fall Meeting, San Francisco, CA, December 2014 .

Budny, M, and BW Benscoter. "Impacts of willow invasion on vegetation water and carbon exchange in the Florida Everglades." American Geophysical Union Fall Meeting, San Francisco, CA, December 2014.

Watts, A., MR Turetsky, BW Benscoter, SE Page, G Rein, and G van der Werf. "Global perspective on peat fires." American Geophysical Union Fall Meeting, San Francisco, CA, December 2014.

Benscoter, BW, and D Harshbarger. “Community carbon exchange along an ecosystem hydrological gradient in the Florida Everglades.” Joint Aquatic Sciences Meeting, Portland, OR, May 2014.

Benavides, V, D Harshbarger, and BW Benscoter. “Ecosystem carbon exchange across a depressional marsh ecotone in Central Florida.” Joint Aquatic Sciences Meeting, Portland, OR, May 2014.

Organized Symposia:

“Carbon storage and release in low latitude peatlands” American Geophysical Union Fall Meeting, San Francisco, CA, December 15-19, 2014 (Co-Conveners: Benscoter, Comas, Hinkle, and Shoemaker)

“Carbon storage and release in low latitude peatlands” Greater Everglades Ecosystem Restoration Conference, Coral Springs, FL, April 23-25, 2015 (Co-Conveners: Comas, Warren, and Benscoter)

“Coastal and Inland: Carbon, water, and energy cycling in a changing environment” Society of Wetland Scientists Annual Conference, Providence, RI, May29-June 3, 2015 (Co-Conveners: Benscoter, Jones, and Shoemaker)

New Notes Concerning the Project

Personnel:

One PhD student (Matt McClellan) has continued his appointment as a research assistant in the Environmental Geophysics Lab at FAU (Comas). During Year 2 of his appointment Matt has focused on completion of fieldwork at DWP and preparation of a manuscript exploring the use of geophysics for better understanding the contribution of depressional wetlands to overall C stock in DWP. He has also conducted a laboratory study to explore differences in gas dynamics (i.e. biogenic gas emissions and production) from peat monoliths extracted from sites at DWP and Blue Cypress. This work has resulted in several published abstracts as detailed above.

One PhD student (Matt Sirianni) has initiated his research exploring the effect that changes in temperature and salt water intrusion may pose on carbon-based biogenic gas dynamics in peat soils using hydrogeophysical methods. Matt is currently further developing the details for his PhD thesis proposal but is already conducting laboratory experimentation on monoliths extracted from the sites investigated in this project.

One Master’s student (Michelle Budny) has completed her thesis research in the Benscoter lab quantifying plant photosynthetic capacity and transpiration as well as the consequences of shrub invasion of sawgrass wetland communities on microclimate and ecosystem water exchange. Michelle will defend her thesis on April 1, 2015, and anticipates graduation in May 2015.

One Master’s student (Tristan Froud) has commenced his thesis research in the Benscoter lab quantifying methane dynamics along the soil-water-atmosphere continuum at Blue Cypress Marsh. Additionally, one

PhD student (Jessica Dell) has commenced her graduate program. While her project is still under development, she will be investigating climate-related resilience of peat-forming wetlands.

One Master's student (Cali Munzenrieder) has initiated her research in the Environmental Geophysics Lab (Comas) exploring the use of capacitance probes to better constrain the temporal resolution of methane and carbon dioxide fluxes from peat soils as well as production within the soil matrix.

Eleven undergraduate students (Stephen Staudt, Emily Persico (UF), Victor Benavides, Jaci Roberto, Nadia Abouhana, Amira Bahhur, Joanne Pauyo, Sebastian Polanco, Michael Eunson. Alex Garcia and Reni Kunkel) have participated in research activities, two of which have conducted independent research projects.

In 2014, co-I Benscoter was awarded Florida Atlantic University Researcher of the Year for the Assistant Professor category and became a National Academies Education Fellow in the Life Sciences. Benscoter was also appointed Chair-Elect of the Society of Wetland Scientists Peatland Section after serving as Chair of the Biogeochemistry Section, and as the Local Host Chair for the Ecological Society of America (ESA) Conference Committee for the 2016 annual meeting to be held in Ft Lauderdale, FL.

Associated Projects:

Dr. Frank Day of Old Dominion University has determined ground-penetrating radar (GPR) protocols for assessing root biomass in longleaf pine through a series of experiments conducted in Virginia. These protocols were tested independently on sites in Florida – one a former elevated CO_2 experimental site at Kennedy Space Center and the other involving a large scale evaluation of carbon pools and climate change in the Everglades watershed (Disney Wilderness Preserve). At the DWP, the following protocols were followed. A dielectric calibration station was established near the eddy flux tower by burying 4 aluminum rods at 4 different depths. Each day that GPR measurements were made soil moisture and soil dielectric constants were determined at the calibration station. Twenty five circular spots (15 cm in diameter) representing a range of root densities were located near the eddy flux tower. These locations were scanned with GPR and then cored to 60 cm depth. The roots were extracted by sieving, oven dried and weighed. These data were then used to establish regressions between root biomass and pixel counts obtained by GPR so that biomass in sample plots could be estimated indirectly with GPR data. Scans of twelve 0.25 m2 plots located in 12 of the University of Central Florida pine flatwoods plots were conducted. The regression equations will be used to estimate root mass in the plots from GPR pixel counts. Each 0.25 m2 plot was then excavated to 60 cm depth and roots removed by sieving, oven dried and weighed. Estimated root mass will be compared with actual root mass in the plots.

Dr. Paul Dijkstra of Northern Arizona University received an Environmental and Molecular Science Laboratory (EMSL-DOE) User Proposal award to investigate biochemical processes associated with microbial biosynthesis and energy production. Dr. Dijkstra continues work along his interest in biochemical processes associated with microbial biosynthesis and energy production. Although these processes are known for single species under laboratory (or industrial) conditions, they are unknown for microbes in real communities, such as soils and sediment. Our research approach is to add position specific 13C-labeled substrates to soil of long-leaf pine flatwoods and marsh sediment and measure how 13CO2 is released from specific atoms within the tracer molecules. The position dependent pattern of CO2 release helps us model how microbes break down for example glucose. In this project, we will

combine the metabolic tracer probing method with other methods, such as metagenomics, metatranscriptomics, metaproteomics, and metabolomics to get detailed information on the microbial community composition and functioning. We have chosen to study the long-leaf pine and marsh because the metabolic processes in these two environments are expected to be very different. The outcomes of this study will help us fine-tune our techniques to understand microbial processes in real communities, and will find applications in a variety of fields, including modeling of soil processes in response to climate change, evaluating agricultural management practices, and generally better understanding the importance of microbes for life on earth.

The researchers, Shannon Hagerty (master student) and Paul Dijkstra (Associate Research Professor) are from Northern Arizona University, and are collaborating with Prof Dr Ross Hinkle, Dept Biology University of Central Florida. The UCF project is funded through a Department of Energy award to Dr. Ross Hinkle, while the specific work in this collaboration is funded with NSF support and through an Environmental and Molecular Science Laboratory (EMSL-DOE) User Proposal award to Paul Dijkstra.

Dr. Chongxuan Liu of Pacific Northwest National Lab is using the DWP site to evaluate the application of the unified multi-scale model. The approach was first developed and applied in the pore-to-core scale system, which is described in a previous paper (Yang et al., 2014). The approach treated surface water flow and groundwater flow as a single flow system and simulated by the same set of equations. This facilitates the modeling of soil water saturation, draining, inundation, etc, which is a very difficult problem using traditional methods, especially at wetland. We will add a biogeochemical reaction module in the code so that we will be able to simulate coupled hydrological processes with organic carbon degradation, CO_2/CH_4 flux, etc. The advantage of the approach is that the same model can be used for systems at different scales from the pore-to-core-to-ecosystem scales. This way, the understanding and knowledge generated from laboratory studies can be readily evaluated and tested at field sites.

A paper was submitted and accepted for this work (see below).

PNNL's TES Research at DWP: VL Bailey (PI), BP Bond-Lamberty (Co-I), C Liu(Co-I)
The Disney Wilderness Preserve (DWP) in central Florida is used as an example of a low-latitude watershed typical of understudied subtropical/peatland ecosystems. The natural hydrologic gradient at the site allows PNNL researchers to study the effects of water saturation on the balance between CO2 and CH4 emissions from soil columns. Soil cores from DWP have been sampled and transported to PNNL for controlled laboratory incubations focused on identifying products, processes, and rates of SOM transformation and CO2/CH4 emissions. These cores were sampled across a moisture/drainage gradient at DWP. Sequential, 30-cm long (10-cm diam) cores were sampled from the surface to critical depths ranging from 1 m to >2 m, depending on transect position. These soil cores have been treated with CH4 percolation, and during incubation CO2 and CH4 evolution were monitored in conjunction with sampling differently-sized soil pore domains to identify differences in the soil solution chemistry associated with these different pores. The incubation is complete, but the experiment is ongoing, with C analyses coordinated in EMSL initiated in March 2014. This work and collaboration continues.

References:

Comas, X., and L. Slater (2007), Evolution of biogenic gasses in peat blocks inferred from non-invasive dielectric permittivity measurements, *Water Resources Research, 43*, W05424.

Comas, X., and L. Slater (2009), Non-Invasive Field-Scale Characterization of Gaseous-Phase Methane Dynamics in Peatlands Using the Ground Penetrating Radar (GPR) Method:, in *Carbon Cycling in Northern Peatlands*, edited by A. Baird, Belyea, L., Comas, X., Reeve, A. and Slater, L., pp. 159-172, American Geophysical Union (AGU).

Craft, C. B., and C. J. Richardson (2008), Soil characteristics of the Everglades Peatland, in *The Everglades experiments: lessons for ecosystem restoration*, edited by C. J. Richardson, p. 698, Springer New York.

Oleson, K. W., Lawrence, D. M., Gordon, B., Flanner, M. G., Kluzek, E., Peter, J. et al.. (2010). Technical description of version 4.0 of the Community Land Model (CLM).

Yang, X., Liu, C., Shang, J., Fang, Y., & Bailey, V. L. (2014). A Unified Multiscale Model for Pore-ScaleFlow Simulations in Soils. Soil Science Society of America Journal, 78(1), 108-118.

APPENDICES

Appendix A

Modeling Littoral Zone Vegetation

Emergent Macrophyte Model

Don DeAngelis, July 8, 2014

This is the draft of a report on the emergent vegetation modeling. The purpose is to calculate both the uptake of carbon due to growth and the release due to decomposition, in order to calculate the net storage per unit time. Because landscapes have spatial heterogeneity, the model is spatially explicit with an elevation gradient.

The model is loosely based on the modeling approach of Asaeda and Karunaratne (2000), variations of which are reported on also in Karunaratne and Asaeda (2000), Asaeda et al. (2002), and Tanaka et al. (2004). We also have used information from Coops et al. (2004).

Growth Model

This model describes emergent macrophyte with phenology. Four state variables, biomass of rhizomes (B_{rhi}) , roots (B_{rt}), new shoots (B_{sd}) and adult shoots (B_{ad}) were selected to simulate plant growth, with units of g m^{-2}

$$\frac{\partial B_{ad}}{\partial t} = Ph_{ad} + \lambda B_{sd} - R_{ad} - M_{ad} - \alpha B_{ad} \quad (1a)$$

$$\frac{\partial B_{rhi}}{\partial t} = - R_{rhi} - M_{rhi} - Gm + x\alpha B_{ad} \quad (1b)$$

$$\frac{\partial B_{sd}}{\partial t} = Ph_{sd} - R_{sd} - M_{sd} + yGm - \lambda B_{sd} \quad (1c)$$

(1d)

$$\frac{\partial B_{rt}}{\partial t} = -R_{rt} - M_{rt} + (1-y)Gm + (1-x)\alpha B_{ad}$$

In the above equations, *Ph* represents primary production, *R* is rate of respiration, *M* is mortality rate, λB_{sd} is the rate of transfer of new shoots to adults, αB_{ad} is the rate of transfer of biomass from adults to belowground storage, and *Gm* is the rate of mobilization of biomass from rhizomes to new shoots and roots. Rates have units g m The values *x* and *y* are both fractions (0 < *x*, *y* < 1) representing relative allocation. The functional forms are as follows. See Table 1 for list of all parameters.

Figure 1 shows a schematic of the biomass dynamics. Figure 2 shows the spatial gradient that the model covers, as well as the fluctuating water conditions.

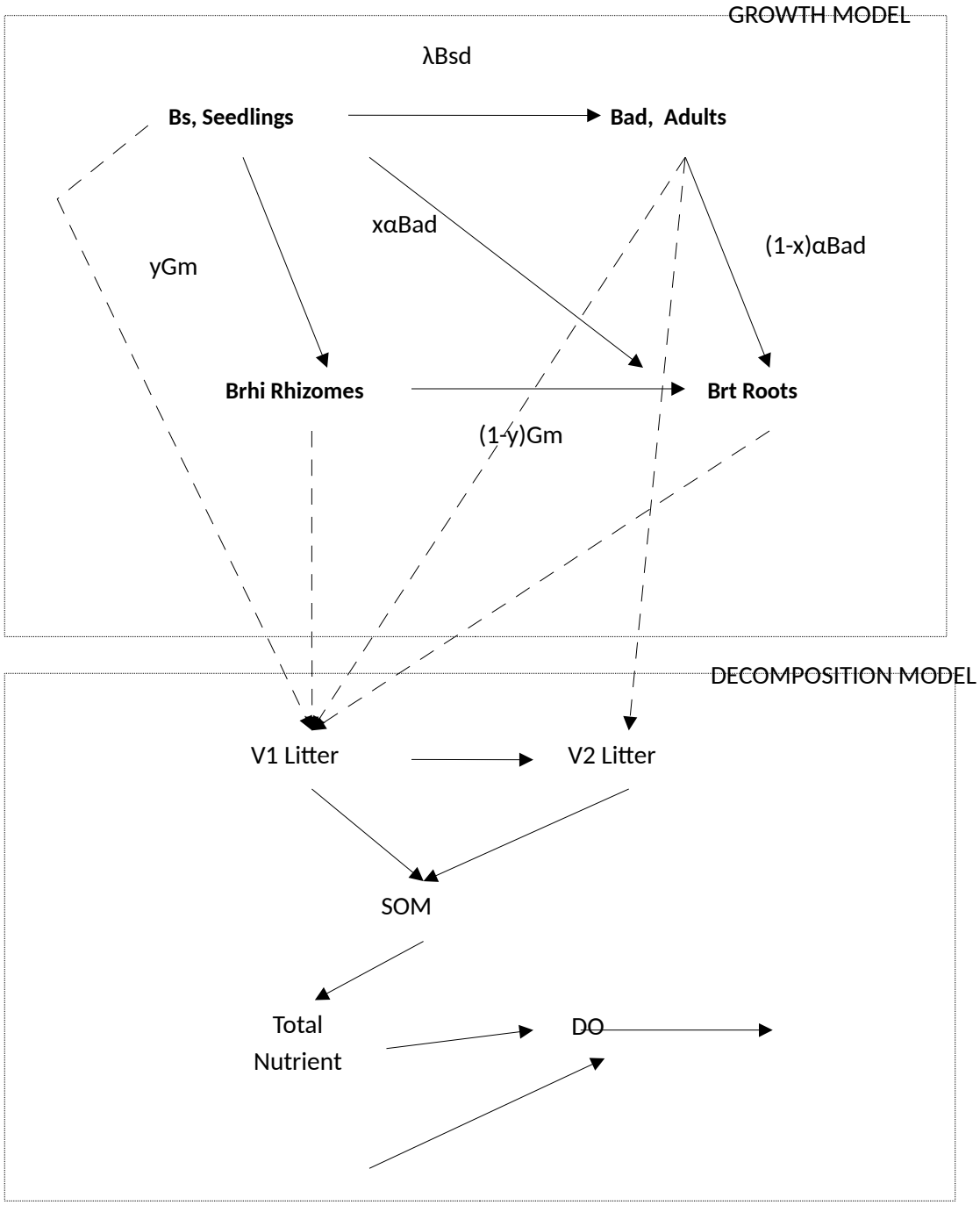

Figure 1. Scheme of emergent plant model

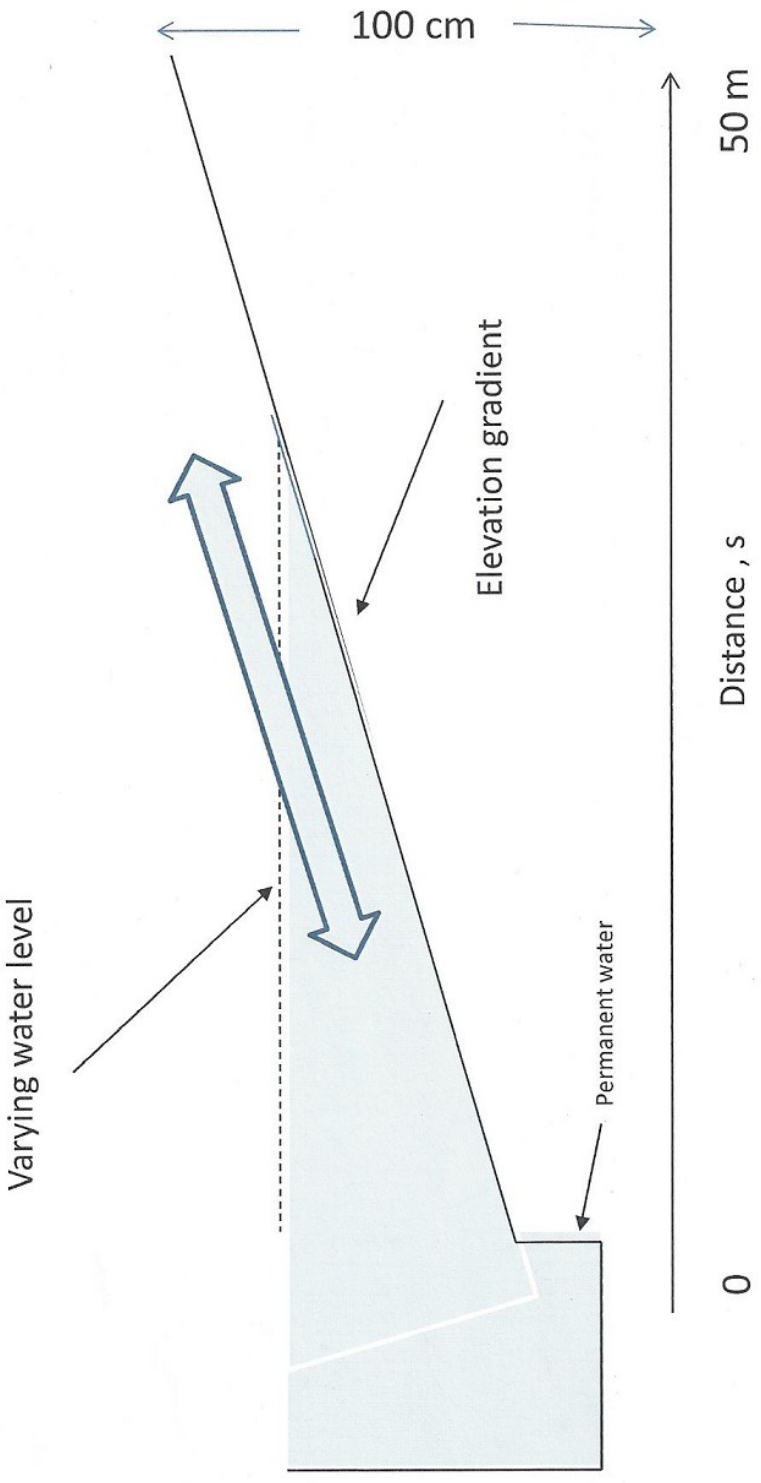
100 cm
50 m
Distance , s
0
Elevation gradient
Varying water level
Permanent water

Figure 2. Schematic of heterogeneous spatial configuration.

Respiration (adult):

$$R_a = \varepsilon_a \theta^{T-20} B_a \quad (2)$$

where θ is the Arrhenius constant and T is temperature.

Mortality (adult):

$$M_a = \eta_a \left(1 + 0.25 e^{0.027 de}\right) B_a, \quad (3)$$

where *de* is water depth.

Mobilization of biomass stored in rhizomes to new shoots and roots:

$$Gm = \beta \frac{1}{1 + 0.15 * e^{-0.5(T-20)}} \rho_{gm} B_{rhi}, \quad (4)$$

Gm is proportional to rhizome biomass, and is affected by temperature and water depth, where ρ_{gm} is water depth limitation of germination. Optimal germination is assumed to occur slightly above water level, germination rate decreases when water depth increases. New shoots can not germinate when water level is too low (Coops et al. 2004). Here, we assume $\rho_{gm} = 0$, when 15cm above water level. To obtain the distribution of germination probabilities, it is assumed that ρ_{gm} follows lognormal function of water level (Figure 2).

$$\rho_{gm} = \frac{1}{b_1 (de + b_3)} exp\left(-\left(ln\left(b_2 (de + b_3)\right)\right)^2\right) \quad (5)$$

A fraction *y*, of *Gm* is allocated to new shoot growth and the rest, 1-*y*, to roots. *Gm* is proportional to rhizome biomass and is affected by daily mean temperature and water level.

Primary production:

Net plant photosynthesis, or primary production, was assumed to be governed by irradiance, mean air temperature, and biomass of the adult shoot.

$$Ph_{ad} = P_{\max}\gamma \frac{1}{1+0.15*e^{-0.5(T-20)}}\left(1-e^{-cI_{PAR}}\right)\frac{B_{ad}}{1+\phi B_{ad}} \quad (6)$$

where I_{PAR} is the mean irradiance absorbed by shoot, given by

$$I_{PAR} = PAR_0\left(1-e^{-kH_{ad}f_{ad}}\right). \quad (7)$$

The exponential factor in (7) represents both absorption of radiation by water and self-shading. We assume only above water level part of shoot can photosynthesize.

$$H_{ad} = \frac{Ha_{max}B_{ad}}{K_{Ha}+B_{ad}} \quad (8)$$

$$f_{ad} = \frac{H_{ad}-de}{H_{ad}}. \quad (9)$$

H_{ad} is the height of the shoot, which can reach a maximum height, Ha_{max}. Note that both primary production and height are saturating functions of B_{ad}.

Model details.

The model simulates energy transport among adults, seedling, rhizome and root. Basic rules are as follows.

Seasonality

1. Rhizomes can transfer energy to seedling and roots, at a rate *Gm*. The rate *Gm* is sensitive to temperature and water depth.

2. The rate *Gm* varies seasonally and is very low, almost zero, at winter. When temperature passes above a critical value, say 10℃, *Gm* increases dramatically until it asymptotes to a plateau.

3. Temperature is read in as monthly means and interpolation is used to obtain values for any particular day.

4. Photosynthesis (*Ph*) has the same response to temperature as *Gm*. Photosynthesis is also density dependent.

5. During winter, due to low temperature, *Gm* and *Ph* are low. Under these circumstances

$$\frac{\partial B_{sd}}{\partial t} = Ph_{sd} - R_{sd} - M_{sd} + yGm - \lambda B_{sd}$$

will be negative, so that biomass of new shoots will decrease.

6. If the contribution of new shoots to adults, λB_{sd}, is small, adults biomass will decrease also. This means $\frac{\partial B_{ad}}{\partial t} = Ph_{ad} + \lambda B_{sd} - R_{ad} - M_{ad} - \alpha B_{ad}$ will be negative, if λB_{sd} =0 during winter. So Ph_{ad} should less then $R_{ad} + M_{ad} + \alpha B_{ad}$, and

$$Ph_{ad} + \lambda B_{sd} < R_{ad} + M_{ad} + \alpha B_{ad}.$$

Water level effects

7. Experimental data show that new shoot germination is high when water level is drawn down. So we assume *Gm* is highest at its optimal water depth, about -5cm (5 cm below soil surface), and decreases when water depth increases, with a long tail following a log normal distribution. *Gm* also decreases when water depth decreases below -5cm, because too low water table will cause emergent seedlings to die. We assume new shoots will not grow when water depth is 15cm below surface.

8. If water depth stays too low, say below -15cm, germination will be stopped. Without an input of *Gm*, $\frac{\partial B_{sd}}{\partial t} = Ph_{sd} - R_{sd} - M_{sd} + yGm - \lambda B_{sd}$ will be negative. Biomass of

seedlings will go towards zero. This will result in $\lambda B_{sd} = 0$ and then adult biomass could decrease, until whole system goes to extinction.

Decomposition Model

Decomposition of leaf and stalk biomass (V_l and V_s , gm^{-2}). These are obtained from

$$\frac{dV_l}{dt} = -(\mu_{1,ae} + \mu_{1,an})V_l + \alpha * V_s + M_{rhi} + M_{sd} + M_{rt}$$

$$\frac{dV_s}{dt} = -(\mu_{s,ae} + \mu_{s,an})V_s - \alpha * V_s + M_{ad}$$

V_l and V_s are represented as daily cohorts of litter, so there should be subscripts ($V_l\ (i)$ and $V_s\ (i)$ where i is the cohort. These are ignored for simplicity

$$\frac{d(SOM)}{dt} = ic(\mu_{1,am}V_l + \mu_{s,an}V_s) - (\mu_{1,ae} + \mu_{1,ae})SOM$$

$$\frac{dTN}{dt} = [nc1(\mu_{1,ae1} + \mu_{1,an})V_l + nc2(\mu_{s,ae} + \mu_{s,an})V_s] + nc1(\mu_{l,ae} + \mu_{l,an})SOM$$

$$\frac{dDO}{dt} = AER - \mu_{l,ae}\beta SOM - \mu_{l,ae}\beta V_l - \mu_{l,ae}\beta V_s - o_n * k_n * TN_{release}$$

where

l = leaf litter, easy to decompose

s = stalk litter, hard to decompose

ae = aerobic

an = anaerobic

SOM = suspended organic matter

TN = total limiting nutrient

DO = dissolved oxygen

nc1 = nutrient to carbon ratios in leaf litter

nc2 = nutrient to carbon ratios in stalk litter

$\mu_{l,ae}$, $\mu_{l,an}$, $\mu_{s,ae}$, $\mu_{s,an}$ = rates of decomposition of leaves (aerobic and anaerobic) and stalks (aerobic and anaerobic).

$\mu_{i1} = \mu_{i1} \max[0,(DO_{water} - 0.1)/(DO_{water} + 0.1)]$

$\mu_{i2} = \mu_{i2} \max[0,(1.0 - DO_{water})/(DO_{water} + 0.1)]$

α = decomposition rate of organic matter from type *s* (hardly degradable) to type *l* (easily degradable)

β = amount of oxygen required to decay 1 g of plant tissue.

ic = anaerobic intermediate organic matter release

Simulation Runs

Typical simulations over a 20 year period are shown in the figures. Temporal values are plotted of rhizomes (B_{rhi}) , roots (B_{rt}), new shoots (B_{sd}) and adult shoots (B_{ad}) were selected to simulate plant growth, with units of g m^{-2} (Figures 1-4). Each of the biomasses in 100 cells along an elevation gradient are plotted. All are started with the same initial values. Temporal values of easily decomposable litter biomass, V_l , and more difficult to decompose biomass, V_s , gm^{-2}, are then plotted (Figures 5-6). The inputs to these are from the mortality of living biomass components.

Note that the easily decomposable biomass, V_l , does not build up over time, but fluctuates seasonally (Figure 5). A fraction of the adult biomass goes into difficult to decompose biomass V_s. This does not reach an asymptote but continues to increase through time (Figure 6). The increase in V_s over time is the carbon that is being stored.

The final biomasses after 20 years are plotted along the elevation gradient (Figures 7-8).

Table 1. Variables and parameters of growth model

Biomass of rhizomes
B_{rhi}

Biomass of seedlings
B_{sd}

Biomass of adults
B_{ad}

Biomass of roots
B_{rt}

Respiration of rhizomes
R_{rhi}

Respiration of seedlings
R_{sd}

Respiration of adults
R_{ad}

Respiration of roots
R_{rt}

Mortality of rhizomes
M_{rhi}

Mortality of seedlings
M_{sd}

Mortality of adults
M_{ad}

Mortality of roots
M_{rt}

Specific dark respiration rate of rhizomes – 0.002
ε_{rhi}

Specific dark respiration rate of seedlings – 0.002
ε_{sd}

Specific dark respiration rate of adults – 0.004
ε_{ad}

Specific dark respiration rate of roots – 0.002
ε_{rt}

Specific mortality rate of rhizomes – 0.000015
η_{rhi}

Specific mortality rate of seedlings – 0.0015
η_{sd}

Specific mortality rate of adults – 0.0015
η_{ad}

Specific mortality rate of roots – 0.000015
η_{rt}

Water depth limitation of germination
ρ_{gm}

Water depth
de

Constant coefficient of water depth limitation for germination – 0.13, 0.08, 15
b_1, b_2, b_3

Temperature constant – 1.09
θ

Photosynthesis of seedlings
Ph_{sd}

Photosynthesis of adults
Ph_{ad}

Maximum specific net daily photosynthesis rate – 0.27
$P_{\max}$

Specific transfer rate of adult biomass to below ground 0.004
α

Specific transfer rate of rhizome biomass to seedlings and roots – 0.06
β

Conversion constant of carbon dioxide to biomass – 0.65
γ

Photosynthesis active radiation – 10000.
I_{PAR}

Extinction coefficient of PAR
k

x Fraction of adult assimilates translocated for rhizomes, rest for roots – 0.8

y Fraction of Gm allocated for seedling growth, rest for roots – 0.9

λ Specific transfer rater of seedling to adults – 0.0067

ϕ Density dependent coefficient – 0.002

Table 2. Parameter values of decomposition model

$\mu_{l,ae} = 3 \times 10^{-8}$

$\mu_{l,an} = 1 \times 10^{-8}$

-

$\mu_{s,ae} = 3 \times 10^{-10}$

$\mu_{s,an} = 1 \times 10^{-10}$

$\alpha = 1 \times 10^{-10}$

$inc = 10^{-4}$

$nc1 = 0.16$

$nc2 = 0.05$

$o_n = 4.57$

$k_n = 7 \times 10^{-7}$

AER = this is input rate of O_2 . Different assumptions are being made for this.

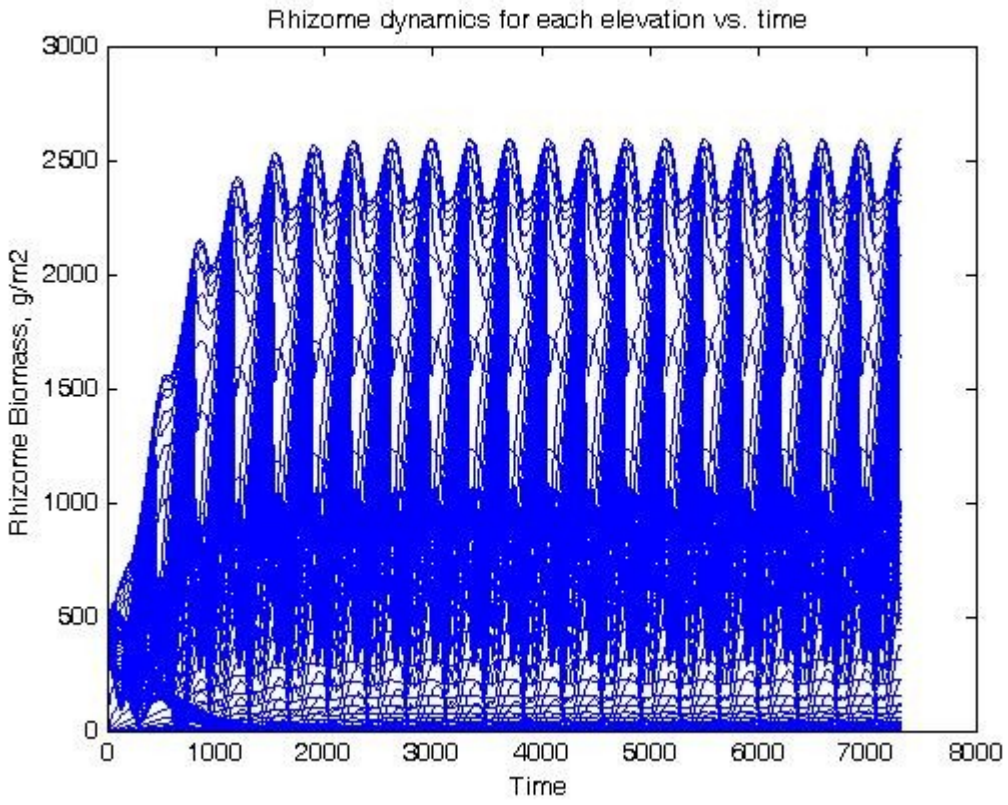

Figure 1. Rhizome biomass in 100 cells along elevation gradient through time

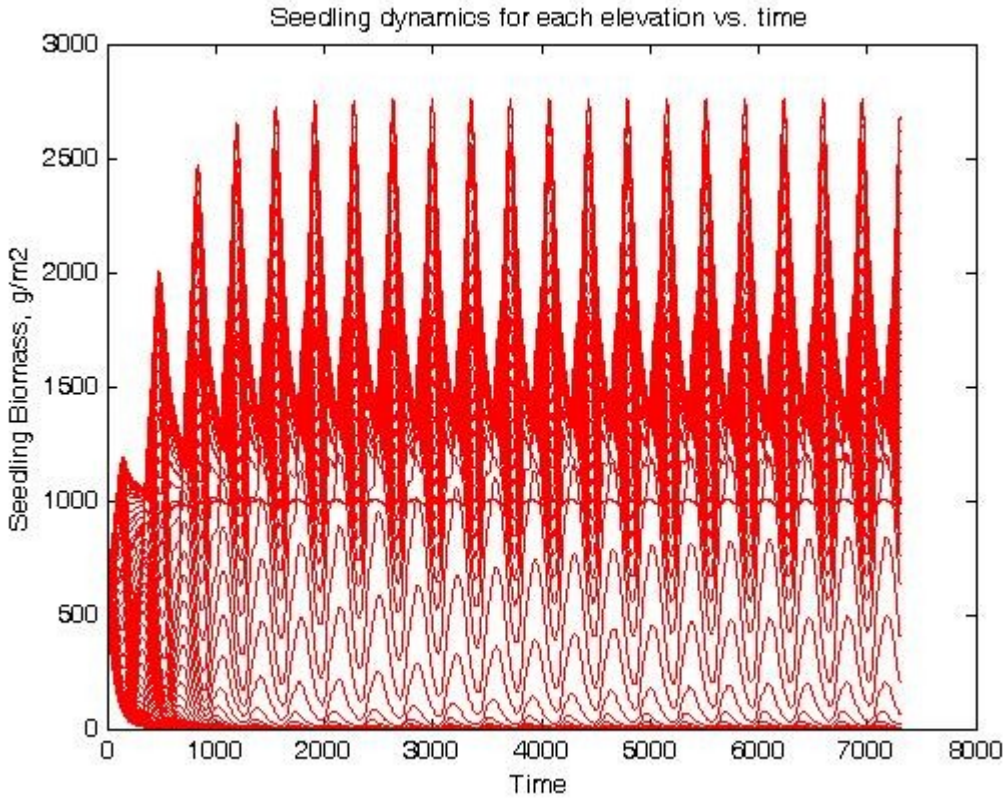

Figure 2. Seedling biomass in 100 cells along elevation gradient through time.

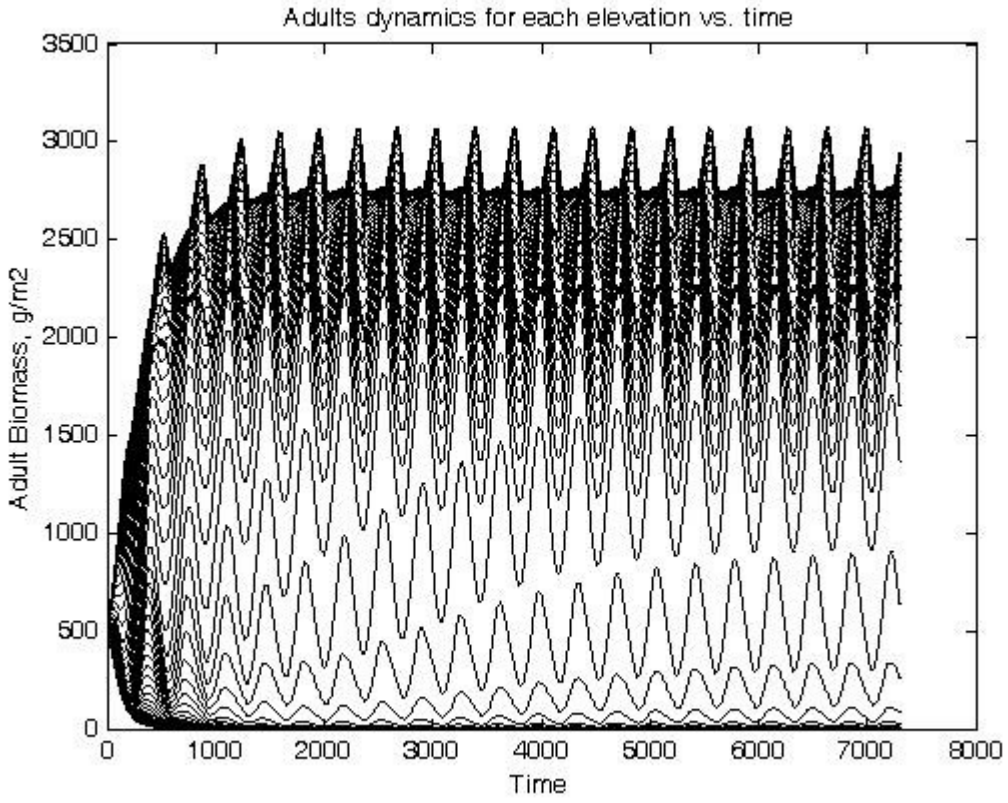

Figure 3. Adult biomass in 100 cells along elevation gradient through time

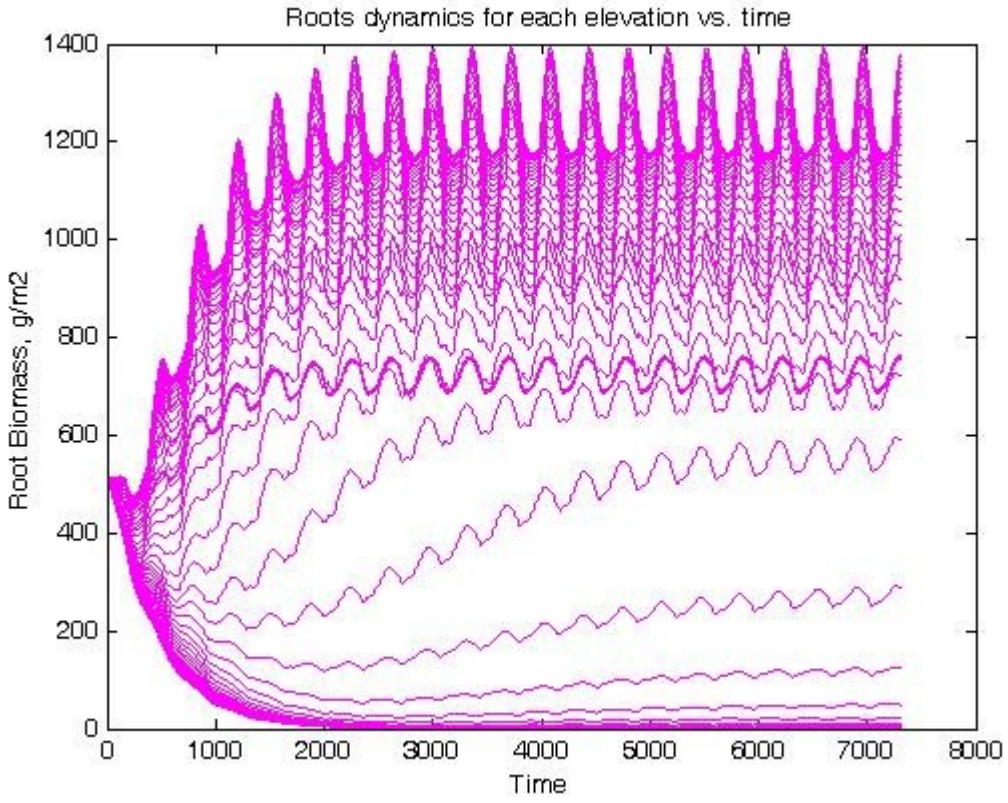

Figure 4. Root biomass in 100 cells along elevation gradient through time

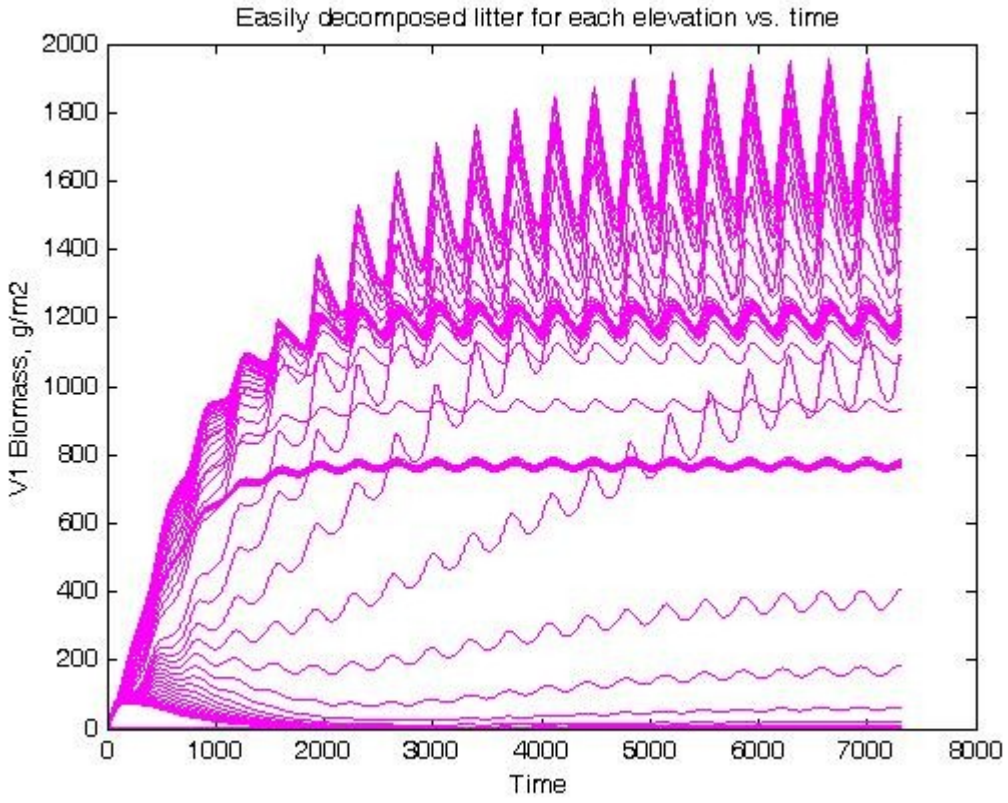

Figure 5. Easily decomposable litter biomass in 100 cells along elevation gradient through time.

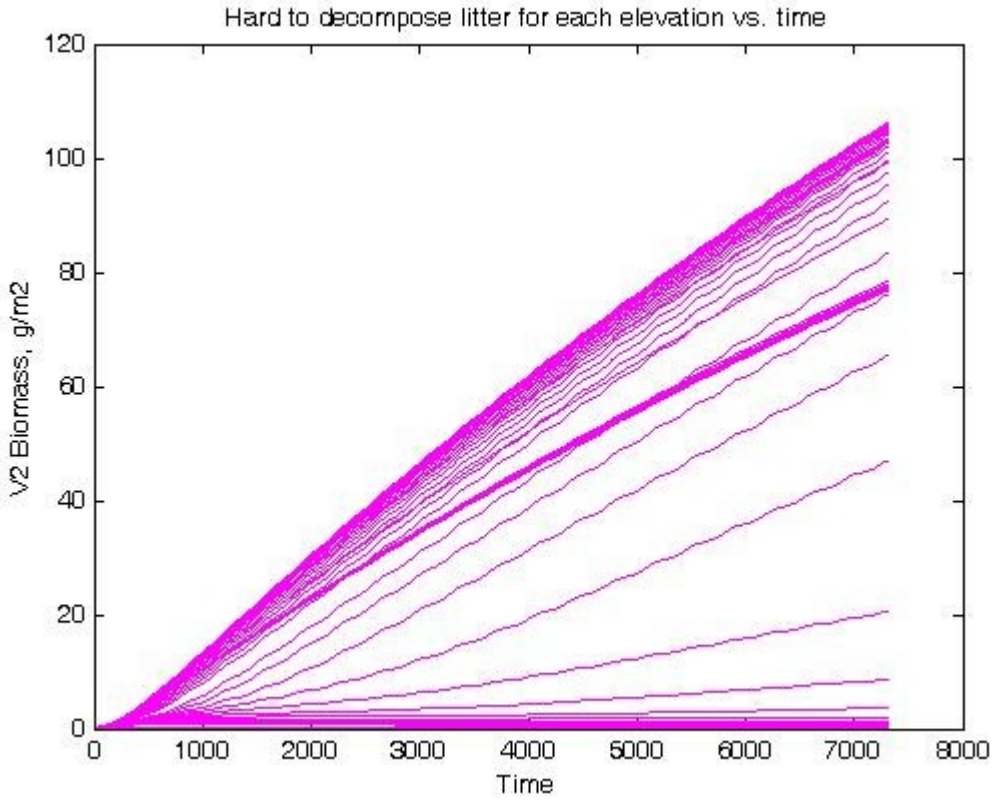

Figure 6. Difficult to decompose litter biomass in 100 cells along elevation gradient through time.

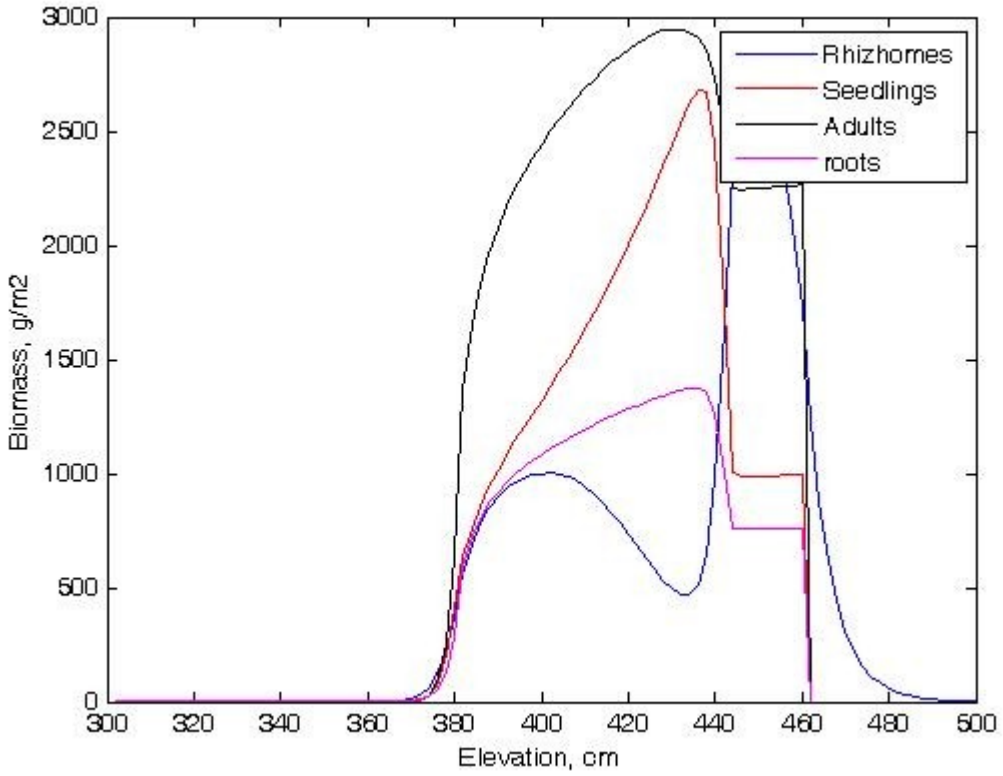

Figure 7. Biomass of living matter along elevation gradient

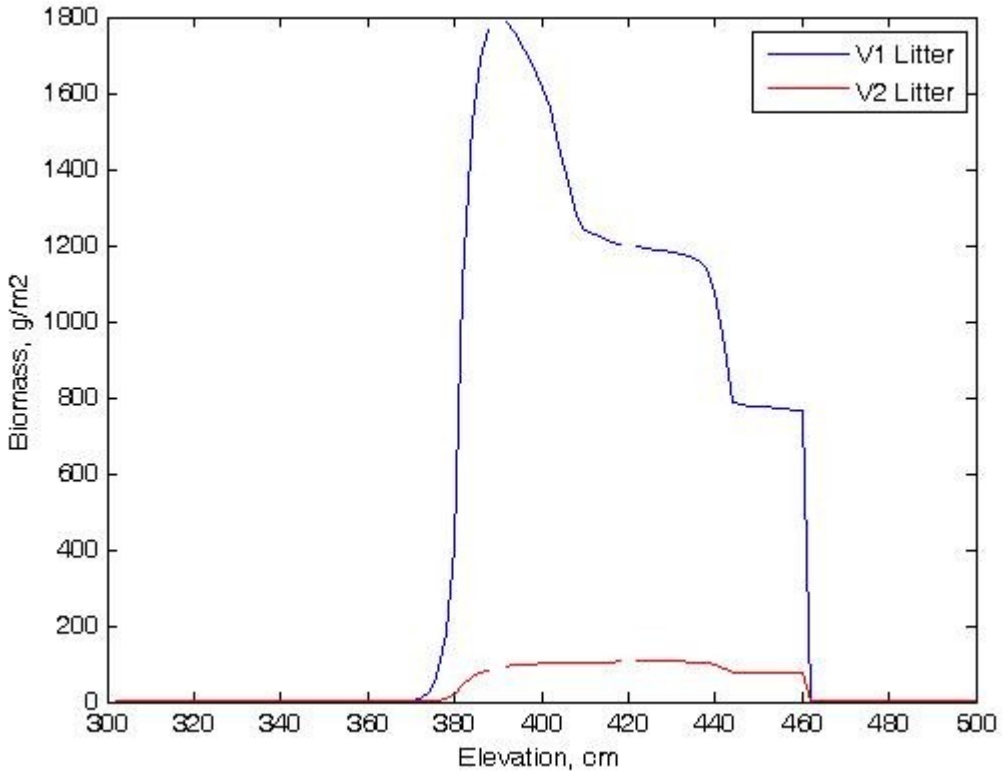

Figure 8. Biomasses of litter along elevation gradient.

References

Asaeda, T. and Karunaratne, S. 2000. Dynamic modeling of the growth of *Phragmites australis*: model description. Aquatic Botany, 67, 301-318.

Asaeda, T., Nam, L.H., Hietz, P. et al. 2002. Seasonal fluctuations in live and dead biomass of *Phragmites australis* as described by a growth and decomposition model: implications of duration of aerobic conditions for litter mineralization and sedimentation. Aquatic botany, 73, 223-239.

Coops, H., Vulink, J.T. and van Nes, E.H. 2004 Managed water levels and the expansion of emergent vegetation along a lakeshore. Limnologica, 34, 57-64.

Coops, H., J. T. Vulink, and E. H. van Nes. 2004. Managed levels and the expansion of emergent vegetation along a lakeshore. Limnologica 34:57-64.

Karunarane, S., and T. Asaeda. 2000. Verification of a mathematical growth model of *Phragmites australis* using field data from two Scottish lochs. Folia Geobotanica 35:419-432.

Tanaka, N., Asaeda, T. Hasegawa, A., Tanimoto, K. 2004. Modelling of the long-term competition between *Typha angustifolia* and *Typha latifolia* in shallow water – effects of eutrophication, latitude and initial advantage of belowground organs.

Appendix B

Modeling Wetland Methane Production and Carbon Storage

(Currently under development by Scott Graham and Don DeAngelis)

Model is being set up from the following papers to simulate simultaneously methane production and carbon uptake in a peatland.

Frolking, S., N. Roulet, and J. Fuglestvedt. 2006. How northern peatlands influence the Earth's radiative budget: Sustained methane emission versus sustained carbon sequestration. Journal of Geophysical Research 11, G01008, doi:10.1029/2005JG000091

Neubauer, S. C. 2014. On the challenges of modeling the net radiative forcing of wetlands: reconsidering Mitsch et al. 2013. Landscape Ecology 29:571-577.

The equations used in the model are (equations 1 and 2) from Neubauer (2014)

$$M_{CH4\text{-}C(t)} = F_{CH4\text{-}C}\,dt + \left[M_{CH4\text{-}C(t\text{-}1)} \times e^{(-dt/\tau_{CH4})} \right]$$

$$M_{CO2\text{-}C(t)} = \sum_{i=1}^{5} \left[f_i (F_{CO2\text{-}C}\,dt + CH4_{ox}) + \left(M_{CO2\text{-}C(t)} \times e^{(-dt/\tau_{CO2,i})} \right) \right]$$

where

$M_{CH4\text{-}C(t)}$ = Inventory of atmospheric methane

$M_{CO2\text{-}C(t)}$ = Inventory of atmospheric carbon dioxide

τ_{CH4} = turnover time of methane in the atmosphere

$\tau_{CO4,i}$ = turnover time of carbon dioxide in the atmosphere in different regions (i = 1,..,5)

$F_{CH4\text{-}C}$ = release rate of methane by wetland

$F_{CO_2\text{-}C}$ = uptake (or release) rate of carbon by wetland

$CH4_{ox}$ = oxidation rate of methane to carbon dioxide

dt = time step (fraction of year)

f_i = fraction of CO_2 in each of 5 atmospheric reservoirs

Sequestration of carbon causes a negative radiation forcing (or cooling effect), but some of the CO2 being taken up in the wetland is converted by soil processes to CH4, which has a positive forcing (warming effect). The model is a way of simulating the relationship between the two fluxes, as shown in some output for different parameter values below.

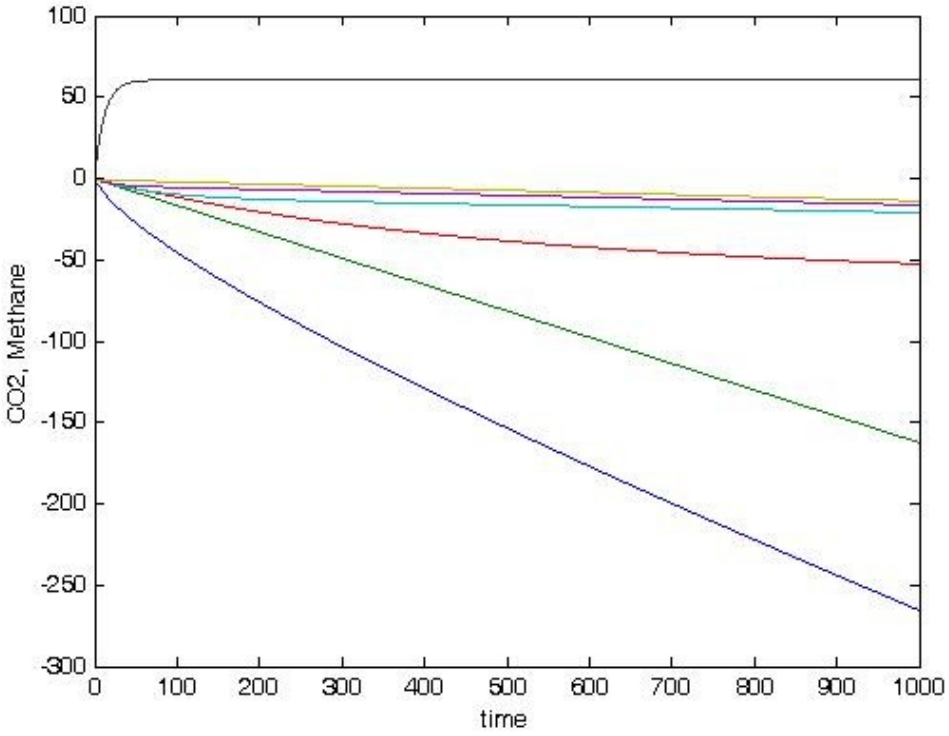

Figure 1. Methane gain (positive) and carbon loss (negative). Carbon losses are divided into 5 atmosphere reservoirs, plus the total (lowest curve). Time is in years.

Figure 1 uses the model and (roughly) the parameters of the papers. The results are qualitatively the same as Figure 1a of Neubauer, and I can also produce the qualitative results shown in Figure 4a of Frolking. But my results deviate quantitatively, because I am not sure what overall multipliers the papers are using to get radiative forcing. Figure 2 (below) uses slightly different parameter values.

This is a start towards more complex simulations that Scott has suggested. These would incorporate the variability in annual CO2 and CH4 flux, and maybe representing periodic fire losses, to predict the long term (centuries to millennia) C sequestration and global warming potential of the wetland.

This would make use of 5 years of eddy covariance data from Blue Cypress marsh which show marsh water level as the main driver of inter-annual variability in CO2 uptake and CH4 emissions. One idea Scott in interested in is how to simulate droughts and fire events

More work to be done on the model to make sure it is working precisely.

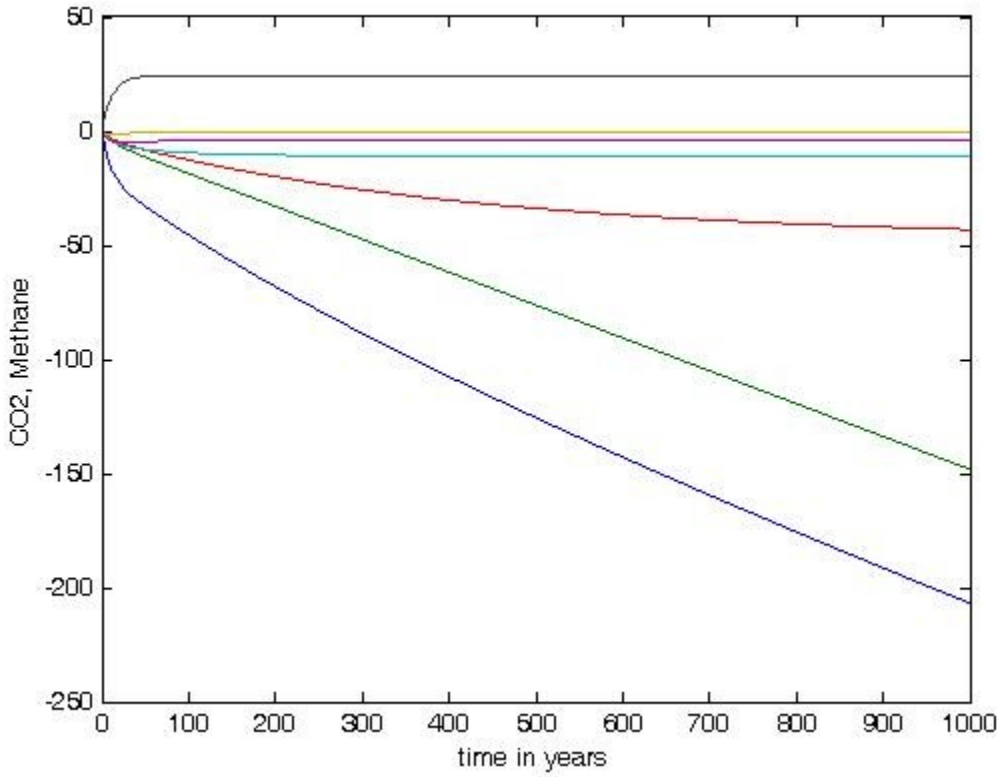

Figure 2. Methane gain (positive) and carbon loss (negative). Carbon losses are divided into 5 atmosphere reservoirs, plus the total (lowest curve). Slightly different parameter values from Figure 1.

Application to Blue Cypress Data

CO2 (g C m-2 y-1) CH4 (g C m-2 y-1) Hydroperiod

2010: -602 33 12-month

2011: -72 26 9-month

2012: -136 32 10-month

2013: -296 45 12-month

2014: -265 (10 months) 26 (10 months) 11-month (fire)

Notes: negative sums indicate net C uptake, positive are emissions. Quantities are in grams C m-2, not g CO2/CH4. Quantities for 2014 are incomplete. A fire in 2014 liberated ~840 g C m-2.

$F_{CO_2\text{-}C}$ = uptake rate of carbon by wetland

= 602 (2010)

= 72 (2011)

= 136 (2012)

= 296 (2013)

$F_{CH4\text{-}C}$ = release rate of methane by wetland

= 33 (2010)

= 26 (2011)

= 32 (2012)

= 45 (2013)

Simulation of 2010-2014. The results for CO2 and CH4 dynamics are shown in Figure 3, and the radiative forcings are shown in Figure 4. I have made an assumption about where the dryouts of the wetlands occurred.

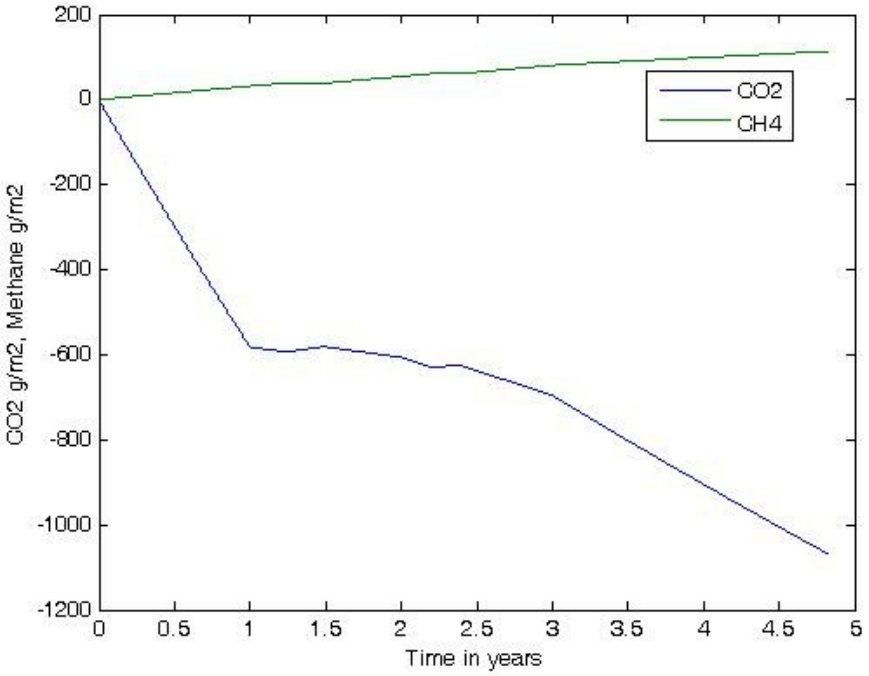

Figure 3. Carbon dioxide loss and methane gain for Blue Cypress data.

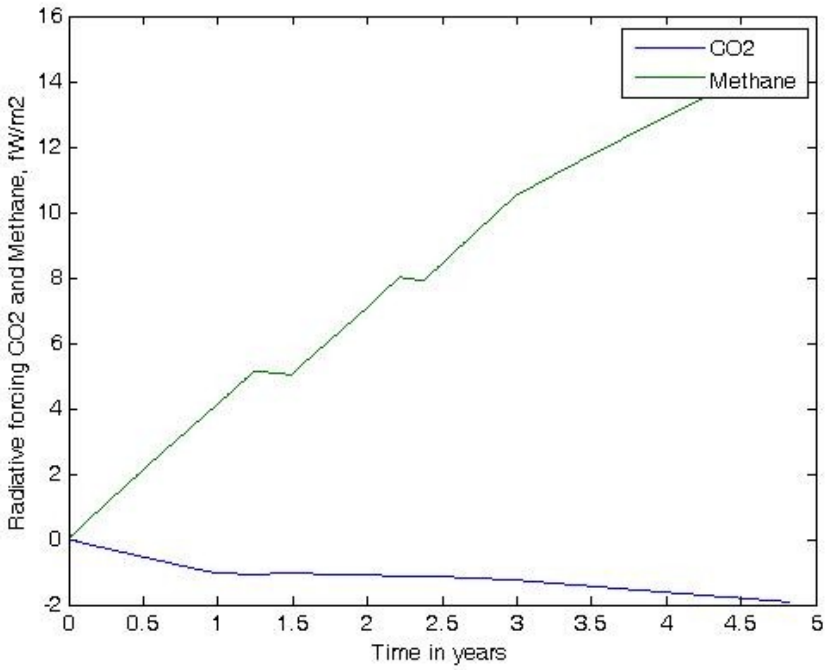

Figure 4. Effects of carbon dioxide loss and methane gain on radiation forcing.

Long-term Simulation

Assuming that the probability of a drought is 0.3 each year. Using the table below (from Hinkle et al. AGU poster 2014) to estimate that the carbon stored during a non-drought year is between 297 and 602, with methane release between 33 and 44, whereas, during a drought year the carbon stored is between 72 and 136, while the methane release is between 26 and 32.

Year	NEP (g C m-2)	RE	GEP	CH4	wl<0 (days)
2010	-602	954	1556	33	0
2011	-72	1247	1320	26	104
2012	-136	1183	1319	32	71

2013	-297	977	1274	44	0
2014	-267 (partial)	936	1202	26	40

Using the probability that there is a fire event on average every 5-8 years (say 0.15 probability per year), with a release of carbon 963 +/- 165 (I am not sure whether there is CH4 release.

Using this approach, the output is shown below from the Frolking/Neubauer model

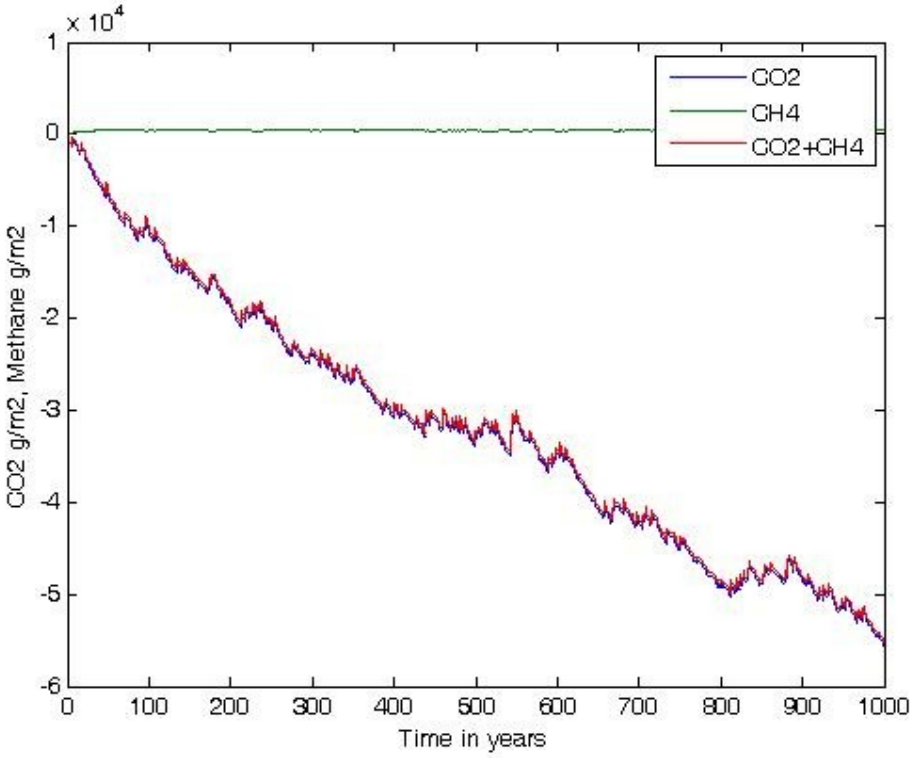

Figure 5. CO2 and CH4 cumulative fluxes.

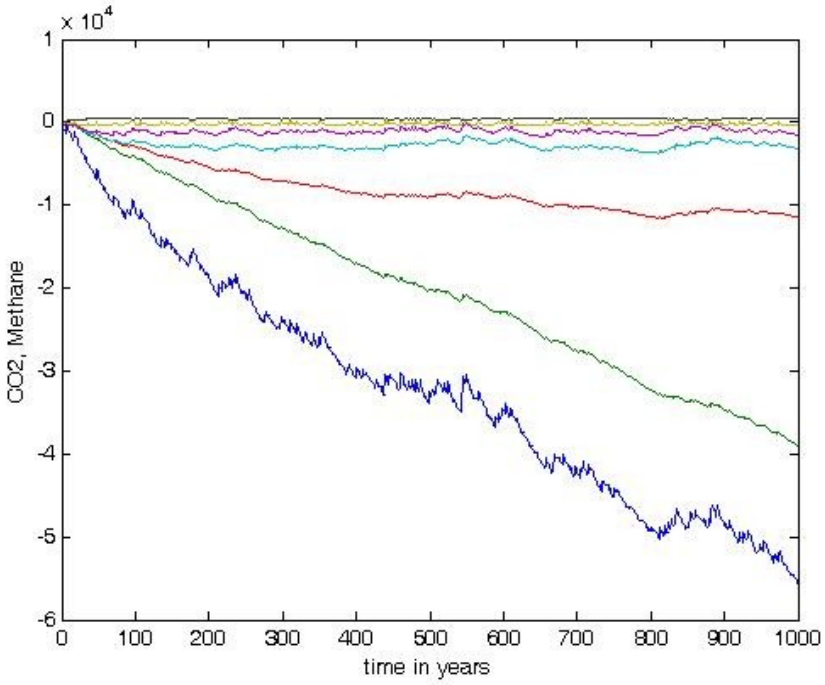

Figure 6. CO2 with atmospheric components

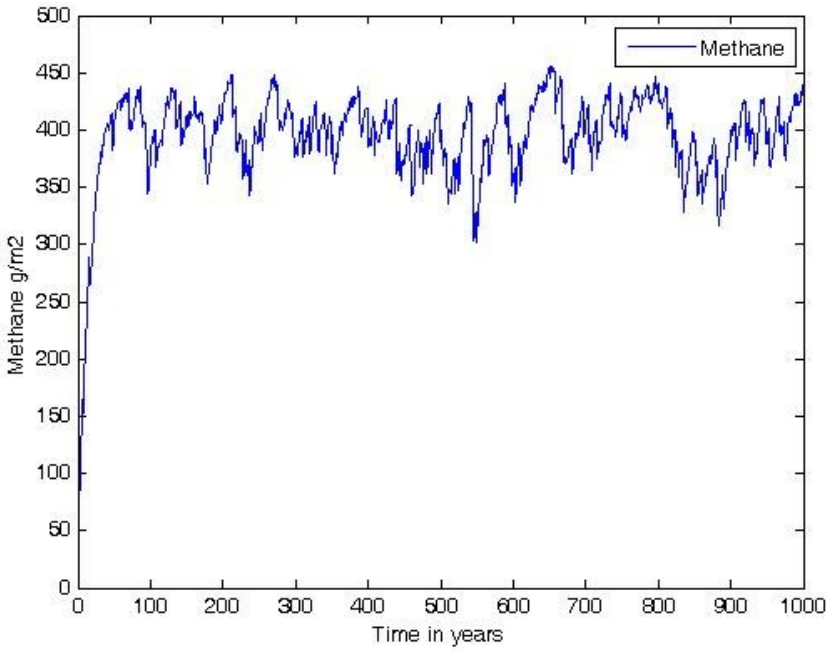

Figure 7. Methane cumulative flux

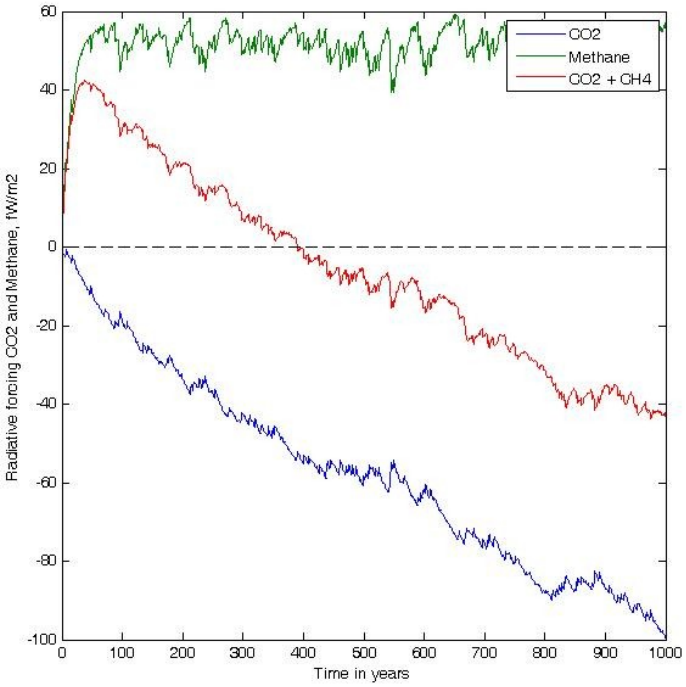

Figure 8. Relative radiative forcings.
Changes in fire frequency:

It is interesting to see the effects of different fire frequencies on the results. Three different probabilities of fire occurring in a given year were run; 1/20, 3/20, and 5/20. The results are shown, respectively in Figures 9, 10, and 11.

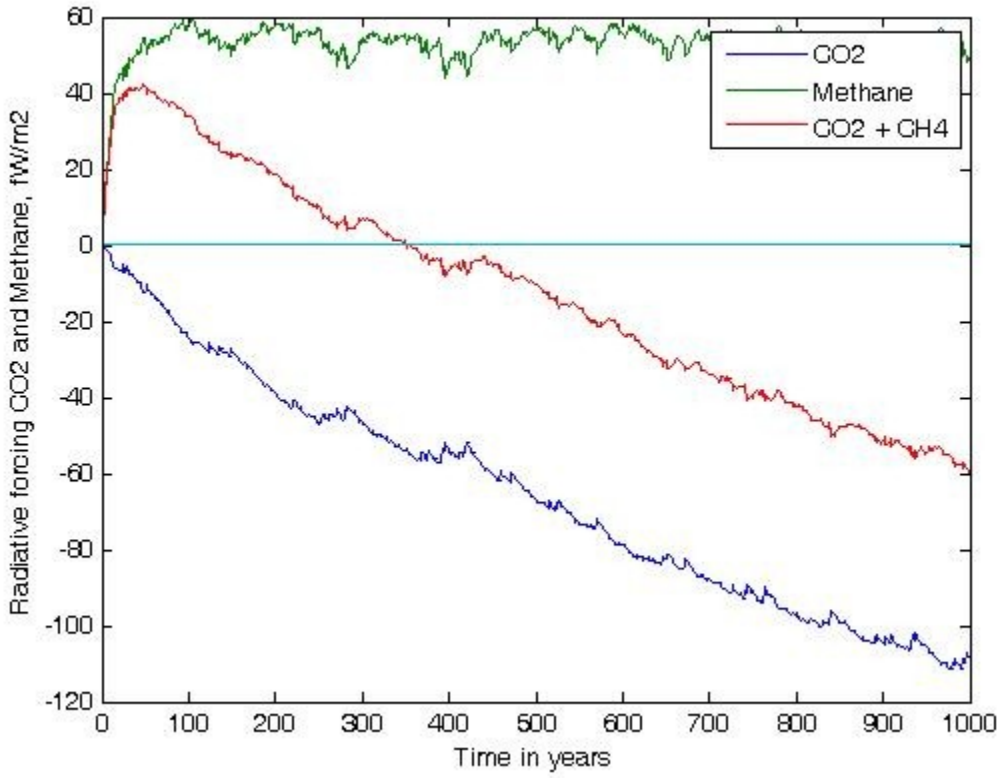

Figure 9. Annual fire probability is 1/20.

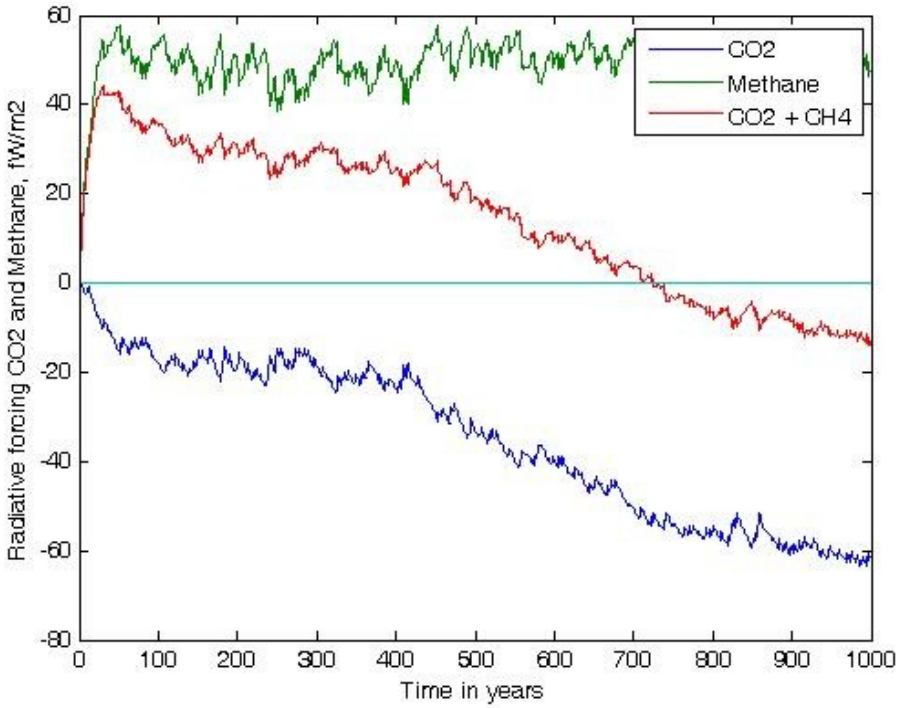

Figure 10. Annual fire probability is 3/20.

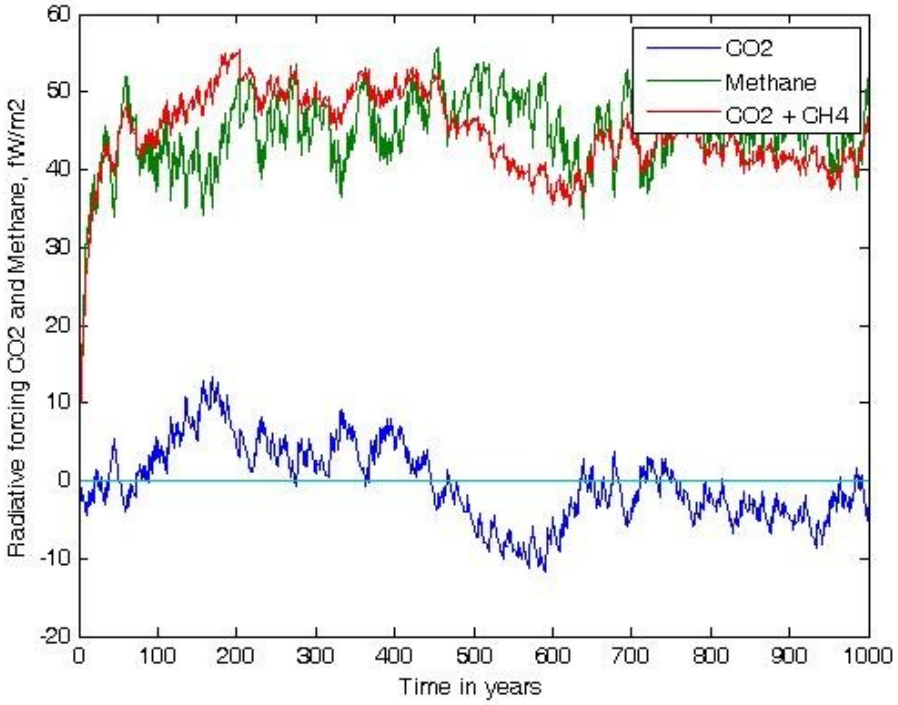

Figure 11. Annual fire probability is 5/20.

(Annual Report 2013-2014)

The Fall 2013 Meeting of the American Geophysical Union provided a good forum to present preliminary results on carbon flux measurements performed at the “wet” (long hydroperiod sawgrass marsh) end of the hydrologic spectrum considered in our study. The citation for the presentation is:

Sumner, David M., C. Ross Hinkle, Scott Graham and Jiahong Li. 2013. Impact of Water Level on Carbon Sequestration at a Sub-tropical Peat Marsh. Eos Transactions of the American Geophysical Union, Fall Meeting, Abstract B21A-0434.

A summary of the presentation is presented below:

Abstract

The impact of water level on sub-tropical peat marsh atmospheric/landscape carbon exchange was explored through eddy-covariance measurement of carbon dioxide fluxes over a site at Blue Cypress Conservation Area in Florida. This site is vegetated with tall, dense sawgrass (*Cladium jamaicense*) and a thick accumulation of peat (over 3 m) suggesting a historically high primary productivity and carbon sequestration. Water managers are particularly interested in understanding how water-level controls can be directed to maintain topography through avoidance of excessive drought-induced oxidative losses of peat soil, as well as to minimize releases of greenhouse gases to the atmosphere. Comparison of net ecosystem productivity (NEP) during a wet year of continuous inundation (680 g C/m^2/yr) and two drier years with 9- and 10-month hydroperiods (111 and 203 g C/m^2/yr, respectively) suggests the positive impact of inundation on sequestration of carbon dioxide. These results are counter to previous research in short stature (1 m or less) sawgrass marshes in the Florida Everglades which indicated suppression of productivity during inundation. This seeming contradiction is probably best explained by the tall stature (over 2 m) of sawgrass at the Blue Cypress site in which inundation does not cover a substantial fraction of the green leaves and the lower (sometimes inundated) canopy is largely composed of brown and decaying leaves. Gross ecosystem productivity (GEP) was suppressed during the drier years (GEP = 1354, 1278, and 1018 g C/m^2/yr for wet, dry, and driest years, respectively), probably as a consequence of canopy moisture stress. Respiration (R) was enhanced for the years when water levels were at times below land surface (R = 674, 1074, and 906 g C/m^2/yr for wet, dry, and driest years, respectively) as a result of soil oxidation. GEP remained suppressed during the dry year even after re-flooding, probably because of relatively low photosynthetic leaf area that was the legacy of reduced canopy growth rates during the drought. The results of this study suggest that water level is a critical control on atmospheric carbon exchanges at this peat marsh with implications for water management and strategic planning under potentially drier conditions that might occur in response to climate change.

Background

A previous study (Schedlbauer et al., 2010) of carbon sequestration at a sawgrass (*Cladium jamaicense*) environment in Taylor Slough indicated that inundation of the surface in this relatively short stature (73 cm) canopy served to suppress net ecosystem productivity, primarily through a reduction in macrophyte photosynthetic activity – in fact, this Taylor Slough site transitioned from a CO_2 sink during periods of

non-inundation to a CO_2 source during inundation. The Blue Cypress sawgrass site that is the focus of the present study provides an opportunity to validate or refine the findings of Schedlbauer et al. (2010) with the important distinction between the Blue Cypress and Taylor Slough sites being the much greater canopy height of the former (200 cm).

Methods

Eddy covariance methods applied to measure CO_2 and vapor (ET) exchanges between atmosphere and sawgrass marsh canopy (half-hour resolution) over 3+ year period (June 2009 – February 2013). Data processing with LI-COR EddyPro software with subsequent u* (>0.15 m/s) filtering of data collected under non-turbulent conditions. Data corrections included: 1) Webb-Pearman-Leuning (WPL) correction for temperature-induced fluctuations in air density (Webb et al., 1980); 2) correction for mis-alignment of the sonic anemometer relative to the ambient airstream (Baldocchi et al., 1988); 3) correction in sensible heat flux computation for error associated with measurement of “sonic”, rather than “actual” air temperature fluctuations (Schotanus et al., 1983); and 4) sensor “frequency response” corrections (Moore, 1986; Moncrieff et al., 1997). Additionally, daily ET was adjusted with an energy-budget closure factor based on the measured Bowen ratio (Twine et al., 2000).

Gap-filling of missing data based on: 1) daytime filling of NEE with light response curve parameterized uniquely for each year-month and 2) nighttime filling of respiration based on a consistent, period-of-record exponential temperature function with a bias-correcting polynomial function of marsh water level . Missing ET data were gap-filled with per year-month parameterized, linear function of net radiation and vapor-pressure deficit.

Results

Roughly 20 and 70 percent of nighttime and daytime, respectively, flux measurements were successful with missing data gap-filled with Equations 1 and 2.

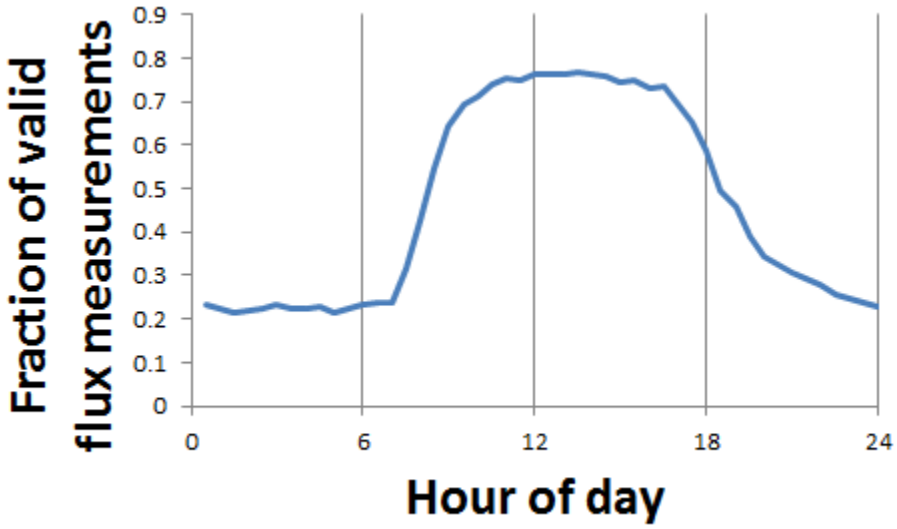

Hydroperiod varied from continuously inundated in 2010 to 9- and 10-month hydroperiods in 2011 and 2012, respectively. Non-inundated conditions occurred during Florida's typical dry Spring period usually peaking in late May.

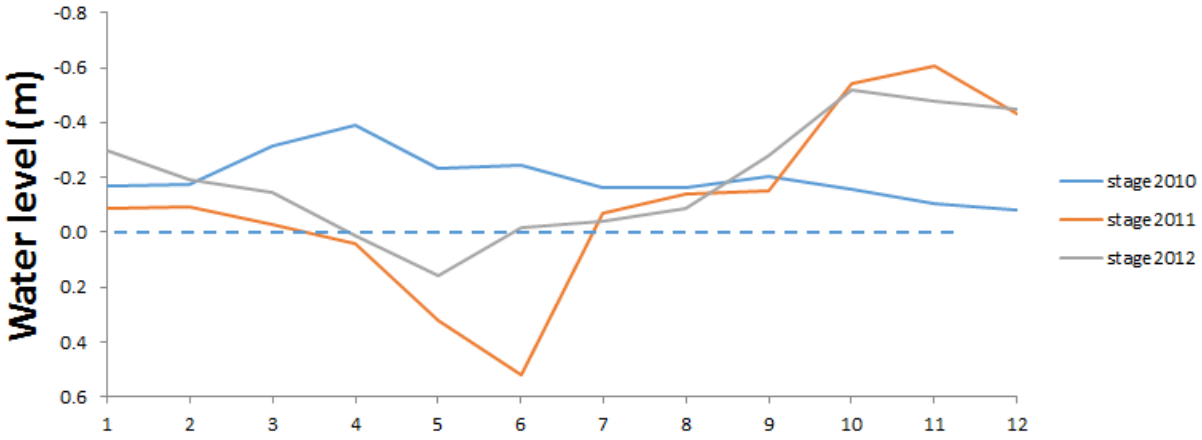

Sequestration decreased with decreasing hydroperiod – counter to results of Schedlbauer et al. (2010) in a shorter stature sawgrass setting.

Legacy impact of late-spring low water levels during drier years (2011/2012) on sequestration later in year, despite water level recovery.

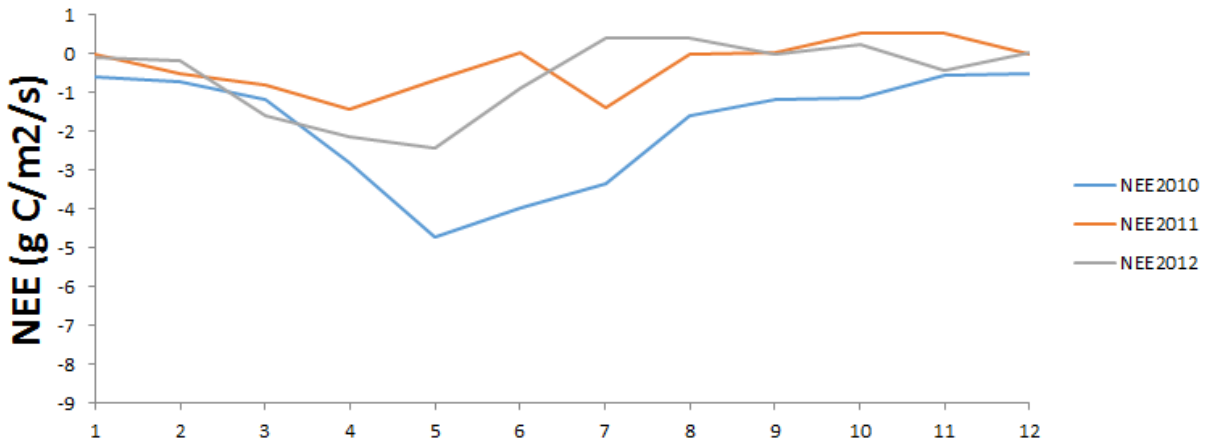

The variation in hydroperiod over the study period had a noticeable impact on carbon sequestration related to both a decrease in productivity and an increase in respiration during dry years.

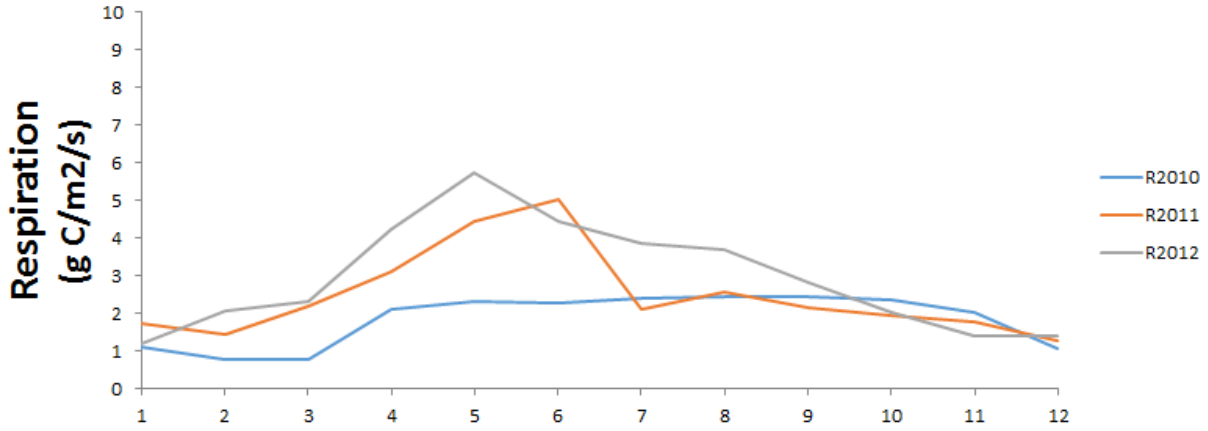

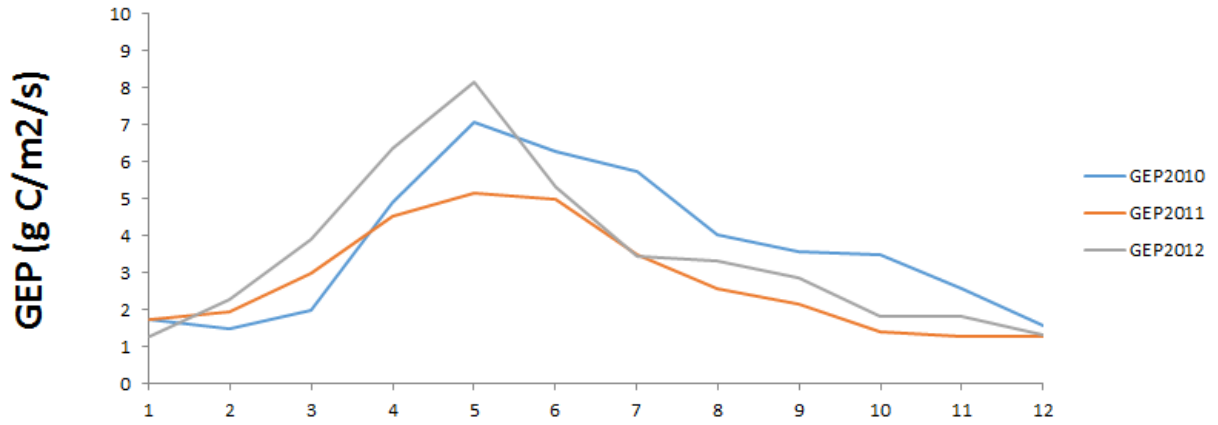

Daytime NEE was well simulated by piece-wise light-response curve.

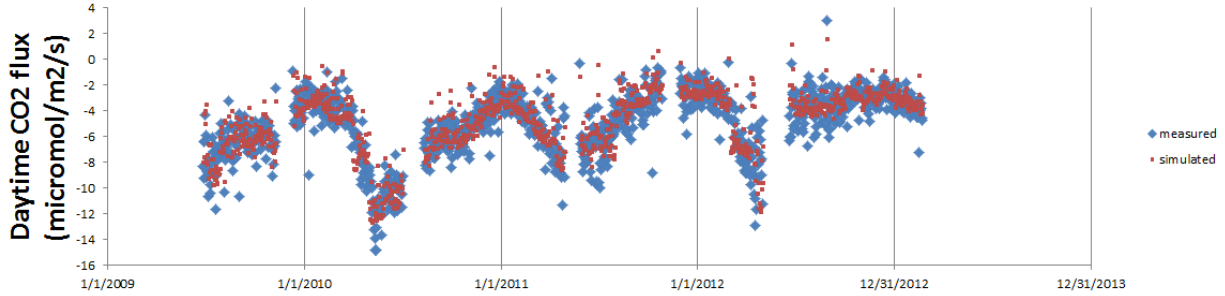

Nighttime NEE was well simulated by a single, consistent exponential temperature function with a bias correction based on water level.

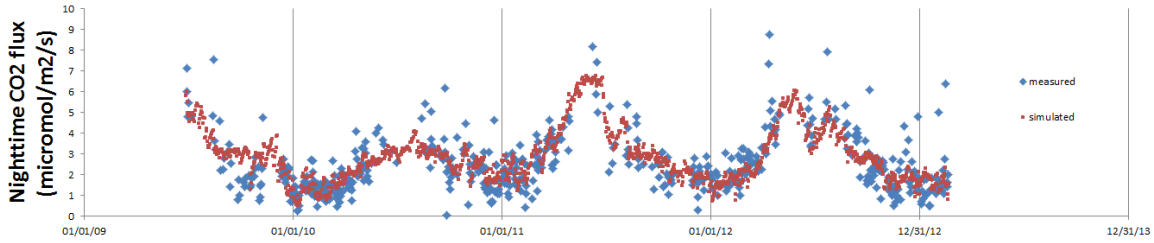

Nighttime respiration was consistently greater than daytime respiration, although the seasonal cycles were similar. Wohlfart et al. (2005) noted the reduction of leaf respiration in light relative to darkness.

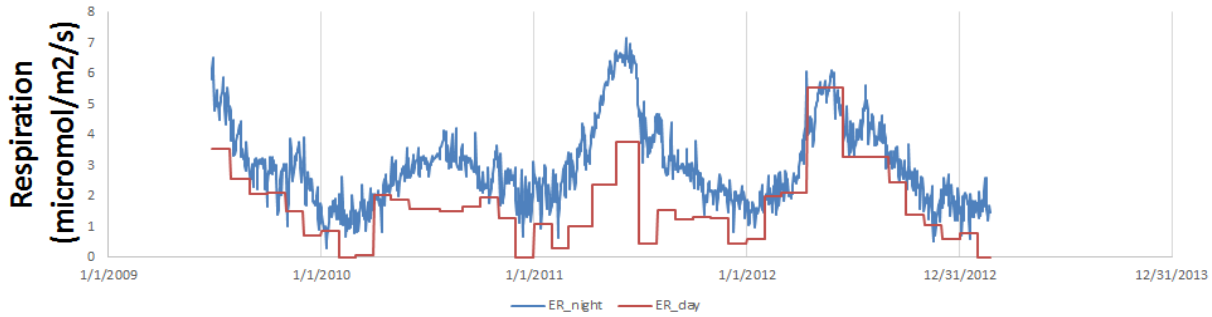

Nighttime respiration was consistently greater than daytime respiration, although the seasonal cycles were similar. Wohlfart et al. (2005) noted the reduction of leaf respiration in light relative to darkness.

Year	Hydroperiod	ET (mm)	NEP (g C/m2)	R (g C/m2)	GEP (g C/m2)
2010	12-month	1,370	-680	674	1,354
2011	9-month	1,287	-111	906	1,018
2012	10-month	1,248	-203	1,074	1,278

Table 1. Summary of annual fluxes of carbon dioxide and water at Blue Cypress marsh; ET = evapotranspiration, NEP = net ecosystem productivity, R = respiration, and GEP = gross ecosystem productivity.

Conclusions

1) Net sequestration of carbon at Blue Cypress marsh is substantial, with annual values ranging from -111 to -680 g C/m^2/yr over three years; respiration is enhanced and productivity suppressed with lower water levels during dry periods.

2) Net sequestration is strongly influenced by hydroperiod, with sequestration of this tall stature sawgrass canopy increasing with hydroperiod – in contrast to a previous study in a short stature sawgrass (Schedlbauer et al., 2010) which showed the reduced sequestration with hydroperiod.

3) Hydroperiod affected carbon sequestration through both a reduction in photosynthesis and an increase in peat mineralization during periods when water level was below land surface.

References

Baldocchi, D.D., Hicks, B.B., and Meyers, T.P. (1988) Measuring biosphere-atmosphere exchanges of biologically related gases with micrometeorological methods. *Ecology,* 69(5): 1331–1340.

Moncrieff, J. B., Massheder, J. M., de Bruin, H., Elbers, J. A., Friborg, T., Heusinkveld, B., Kabat, P., Scott, S., Soegaard, H., and Verhoef, A., 1997. A system to measure surface fluxes of momentum, sensible heat, water vapour and carbon dioxide. *Journal of Hydrology*, 188: 589-611.

Moore, C. J., 1986. Frequency response corrections for eddy correlation systems. *Boundary-layer Meteorology,* 37(1): 17-35.

Schedlbauer, Jessica L., Oberbauer, Steven F., Starr, G., and Jimenez, Kristine L.. (2010). Seasonal differences in the CO2 exchange of a short-hydroperiod Florida Everglades marsh. *Agricultural and Forest Meteorology*, 150: 994-1006.

Schotanus, P., Nieuwstadt, F.T.M., and de Bruin, H.A.R., 1983, Temperature measurement with a sonic anemometer and its application to heat and moisture fluxes. *Boundary-Layer Meteorology*, 50: 81–93.

Twine, T.E., Kustas, W.P., Norman, J.M., Cook, D.R., Houser, P.R., Meyers, T.P., Prueger, J.H., Starks, P.J., and Wesely, M.L., 2000, Correcting eddy-covariance flux underestimates over a grassland: *Agricultural and Forest Meteorology,* 103: 279-300.

Webb, E.K., Pearman, G.I., and Leuning, R., 1980, Correction of flux measurements for density effects due to heat and water vapour transfer. *Quarterly Journal of the Royal Meteorological Society*, 106: 85–100.

Wohlfart, G., Bahn, M., Haslwanter, A., Newesely, C. and Cernusca, A. (2005) Estimation of daytime ecosystem respiration to determine gross primary production of a mountain meadow. *Agricultural and Forest Meteorology*, 130: 13-25.

(Annual Report 2012-2013)

This is the first year of the project, so the information below is related to specific startup progress and efforts related to each objective to date.

Objective 1. Quantify above- and belowground carbon stocks of terrestrial ecosystems along a seasonal hydrologic gradient in the headwaters region of the Greater Everglades watershed.

The Longleaf Pine site has been well characterized with data collection in 47 (meter square) plots to include aboveground biomass, litter, ground cover, and preliminary root cores to estimate belowground biomass and carbon content of the soil. The bulk of this work was started prior to the current project as part of a doctoral dissertation project which will include data from this project (Figure 1). Pre- and

post-fire data have been collected and preliminary analyses have been made to estimate carbon (C) stock. In general we are finding that this ecosystem serves as a net sink of C. However, it became a net source of C immediately following the fire event, with a ~40% loss of aboveground C stock, but recovered to a net sink of C within 6 weeks of the fire (Figure 2). Annually this ecosystem was found to serve as a net C sink even with a prescribed fire event, with annual net ecosystem productivity (NEP) of 508 g C/m^2 in a non-fire year (2010) and 237 g C/m^2 in a fire year (2011). We have continued the eddy covariance measurements at this site and will include all data as part of this study.

Figure 1. Eddy covariance tower in pine flatwoods at Disney Wilderness Preserve.
Photo courtesy of Ben Bon-Lamberty.

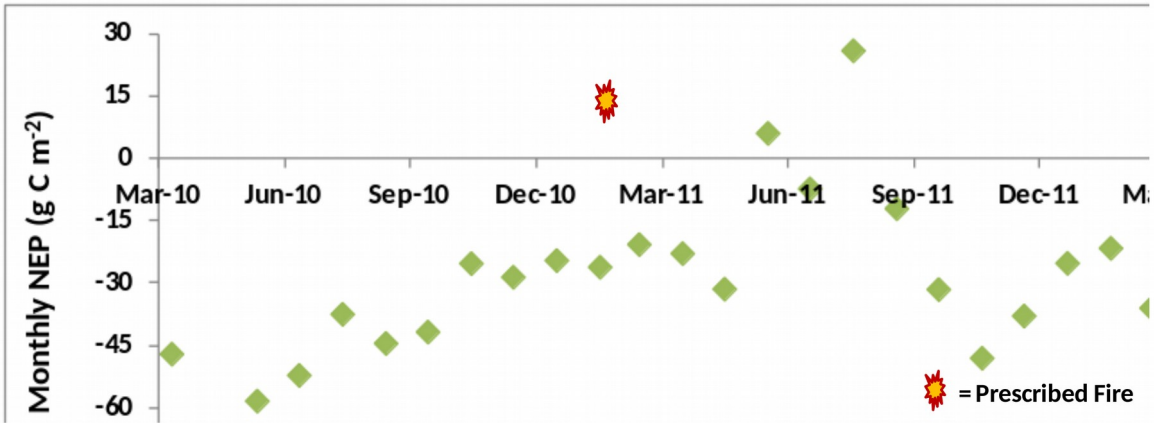

Figure 2. Monthly net ecosystem productivity measured at the pine flatwoods site.

Preliminary ground penetrating radar (GPR) surveys were collected in the pine flatwoods site of the Disney Wilderness Preserve in order to characterize radar facies in the context of subsurface geology and to test the potential of the GPR method for detecting underground roots. A preliminary GPR transect collected (Figure 3) about 100 meters from the eddy covariance tower. The reflection record is characterized by a laterally continuous reflector about 2 meters depth interpreted as the water table. The area immediately above the water table is characterized by a sequence of semi-continuous reflectors and numerous hyperbolic diffractions interpreted as buried roots (as confirmed from the presence of roots at the surface). A hardpan layer characterized by a sequence of wavy reflectors and the presence of diffraction of hyperbolas between 2-5 m depth and a sequence of laterally continuous reflectors at approximately 5 m depth are interpreted below the water table. In order to further investigate root zones above the water table and enhance spatial resolution during surveying, the profile was recollected using higher frequency 250 MHz shielded antennas (Figure 3 inset). The higher frequency results confirm the presence of diffractions extending several meters and interpreted as buried roots. Despite the limitations of these preliminary results, GPR shows promise for imaging the lateral and vertical extent of tree roots in our study site. Future surveys will include extended surveys (both in 2D and 3D mode (following the approach in *Butnor et al, 2001*) in order to characterize the extent of tree roots and associated biomass.

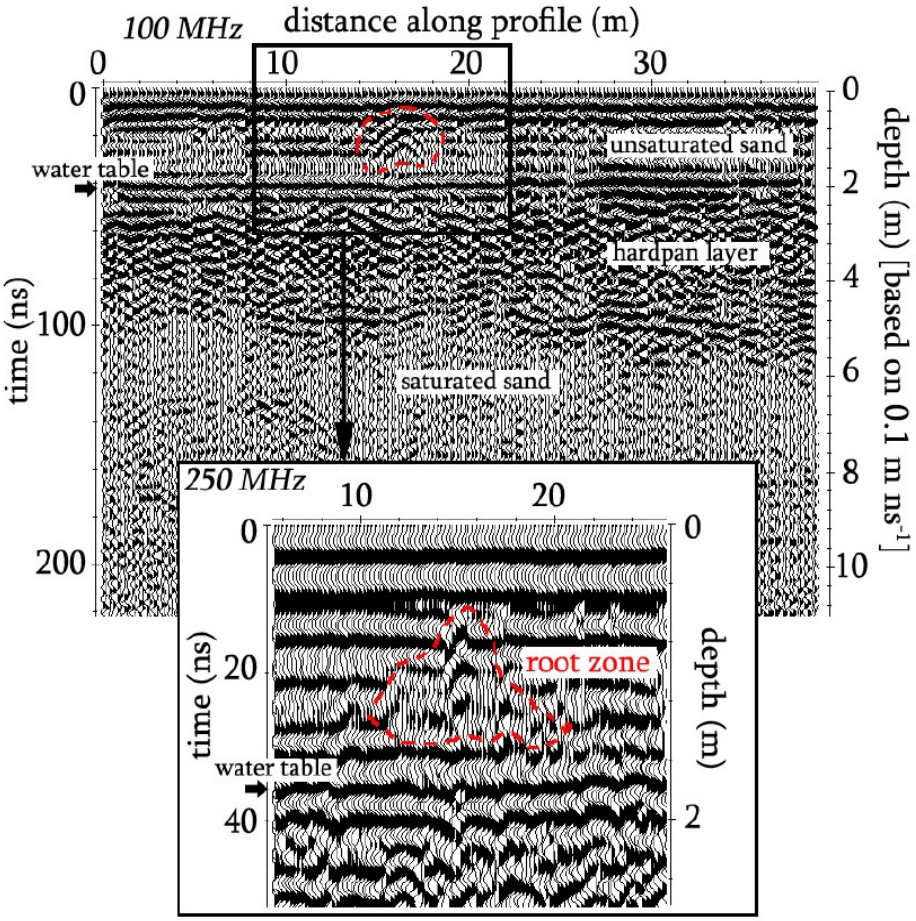

Figure 3: Common offset GPR profile using 100 MHz antennas. Interpreted lithology is constrained from nearby well collected in a previous study. Red line indicates interpreted root zone. Inset shows common offset GPR profile using 250 MHz and interpreted root zone. EM wave velocity used for conversion of depth scale (0.1 m ns^{-1}) was based on estimates from GPR common midpoint surveys.

A set preliminary GPR profiles were also collected at the saw grass marsh site (Blue Cypress) in order to test the ability of GPR to detect changes in peat thickness at large field scales (~100-1000 meters). A GPR common offset profile (Figure 4a) collected near the Blue Cypress Eddy Covariance Tower system (Figure 5) shows the interface peat clay at 3.4 m depth. A set of preliminary surveys using the experimental setup shown in Figure 4c and pulled from an airboat was used to test and prove the ability of GPR to detect changes in peat thickness at large scales (i.e. as shown in the 550 m long transect in Figure 4b).

No carbon stock data has been collected at the depression marsh site to date, but will be collected as we set up the eddy covariance tower and small chambers later this Spring and Summer..

Figure 4: a) Common offset GPR profile using 250 MHz antennas in Blue Cypress showing interface peat-clay. Coring information was collected with a Russian corer; b) variability in peat thickness estimated from changes in depth to the peat-clay reflector; and c) GPR experimental setup in the field.

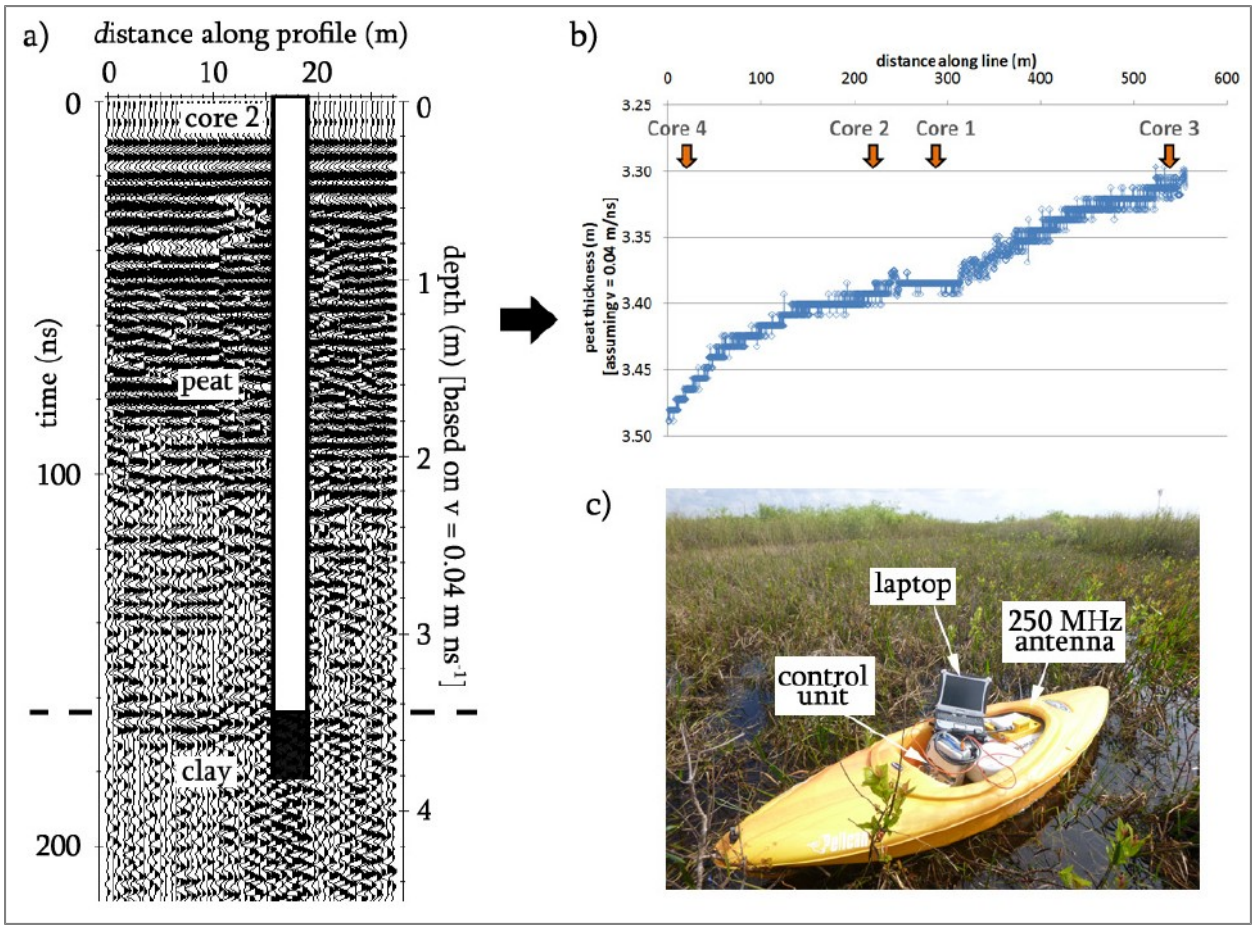

Reference:

Butnor, J.R., JA Doolittle, L. Kress, S. Cohen, and KH Johnsen. 2001. Use of ground-penetrating radar to study tree roots in the southeastern United States. Tree Physiology 21, 1269-1278.

Objective 2. Develop budgets of ecosystem gaseous carbon exchange (CO_2 and CH_4) across the seasonal hydrologic gradient at multiple spatial scales.

We have purchased all the equipment to complete three sets of eddy covariance towers for the longleaf pine, depression marsh, and saw grass marsh. The pine flatwoods site (Figure 1) and saw grass marsh sites (Figure 4) which were in place prior to the start of this project have continued operating with successful data collection. The team has selected the depression marsh site and will be installing the eddy covariance tower there this month (March 2013).

Preliminary time-lapse GPR data for investigation of biogenic gas dynamics have not been collected at this point however measurements will be initiated after preliminary data acquisitioning the depression marsh and are anticipated during the Spring and Summer of 2013. Preliminary designs have been determined for the small chamber soil gas exchange experiments, and those will begin this spring and summer. Dr. David Sumner, United States Geological Survey and Co-PI on this project, has lead the

effort to upgrade our Blue Cypress eddy covariance site. A pre-existing eddy covariance (water vapor and carbon dioxide) station at the Blue Cypress sawgrass marsh (representing the wet end of the hydrological spectrum being studied in this project) has been upgraded to include a Licor 7700 methane analyzer to allow for methane flux measurements and the Licor 7550 logging interface to allow for greater compatibility with contemporary Licor data processing (Figure 5). Operation/maintenance and data retrieval/processing at this station has continued since commencement of project start date (Fiscal Year 2013).

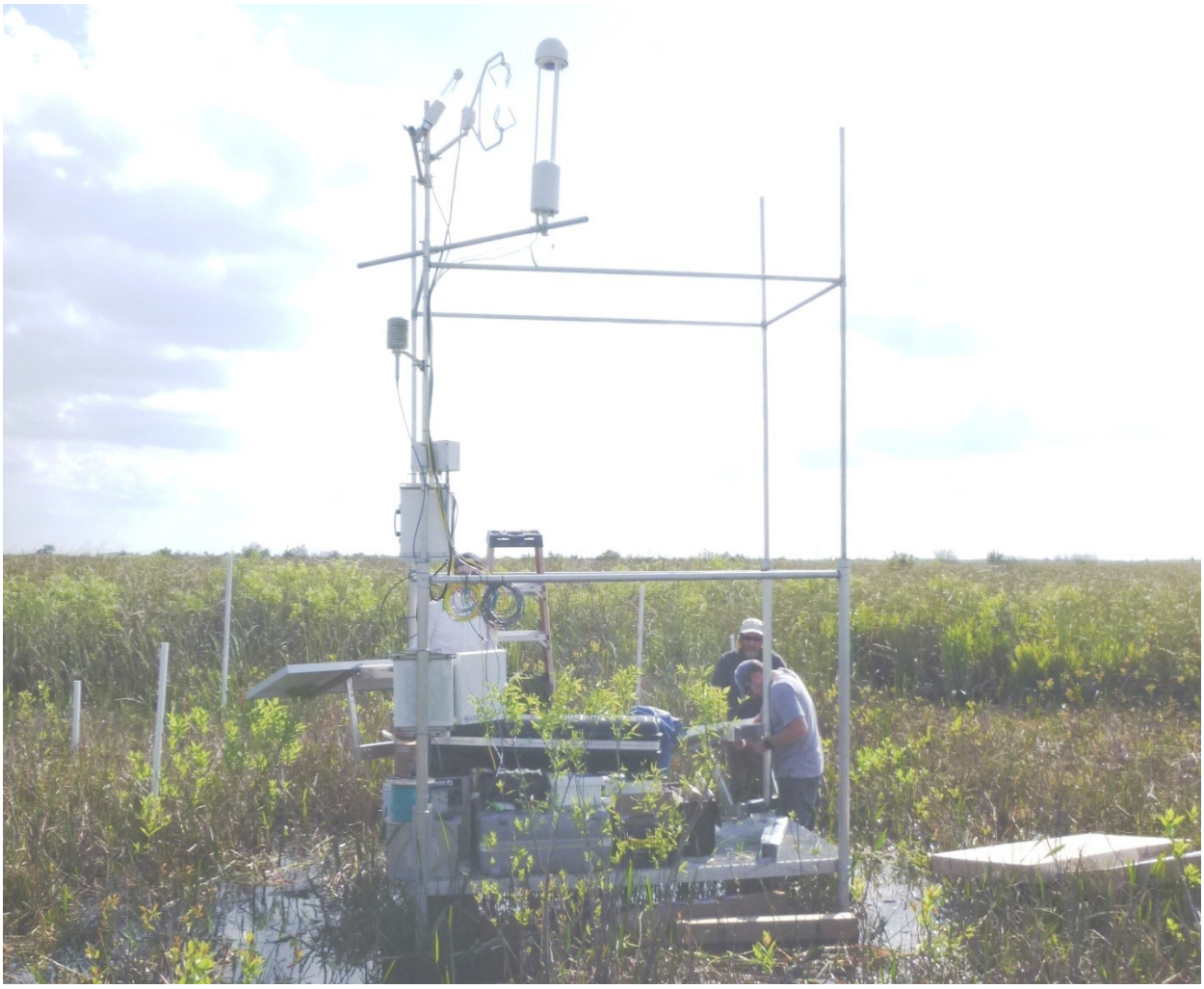

Figure 5. Blue Cypress Eddy Covariance Tower system. (Photo courtesy of Xavier Comas

Objective 3. Assess the impact of climate drivers on ecosystem carbon exchange in the Greater Everglades headwater region.

No activities to date.

Objective 4. Integration of research findings from Objectives 1-3 with climate-driven terrestrial ecosystem carbon models to examine the potential influence of projected future climate change on regional carbon cycling.

Co-investigator Don DeAngeles has developed a preliminary carbon dynamics and sequestration model based upon the G'DAY model (Appendix A). He has begun parameterizing it for the Florida sites.

Papers and Other Products Delivered

The Principal Investigator, Dr. Ross Hinkle was invited to give a seminar in the Department of Biology at Old Dominion University in Norfolk, Virginia on March 08, 2013. The presentation entitled "*Carbon dynamics in selected subtropical ecosystems in Central Florida*" covered research in central Florida for the past 15 years and highlighted the current project as future directions for carbon dynamics research as part of the DOE TES program.

The following published abstract was partially supported by this grant:

Comas, X., Wright, W., Heij, G. Investigating methane flux dynamics in subtropical peat soils of the Everglades using hydrogeophysical methods. Abstract B31D-0456 presented at 2012 Fall Meeting, AGU, San Francisco, Calif., 3-7 Dec.

New Notes Concerning the Project

Two collaborations that are being developed between the PIs of this project and other DOE funded research are being considered to take advantage of the synergy between the research activities and to enhance the overall value of DOE funded research. Dr. Paul Dijkstra, Northern Arizona University, and Dr. Nancy Hess, EMSL, coordinated with the project PIs to establish an opportunity for using the DWP research site for research in an EMSL user's access proposal entitled *"Analyzing soil microbial central C metabolic network processes across a gradient of carbon availability and oxygen concentration in a Florida landscape."* The stated objectives of that collaborative activity are:

1. Determine in detail the make-up of the intracellular and extracellular C metabolites and protein profiles across a gradient of C availability and oxygen concentration and in response to changes in moisture, temperature, litter quality, and N availability.
2. Determine what organic C substrates are consumed and what products are secreted by the soil microbial community. Experiments will use position-specific and uniformly 13C-labeled metabolic tracers at a range of concentrations in short to medium-long soil incubations.
3. Determine members of the soil microbial community that consume the metabolic tracers used in these experiments.

Dr. Vanessa Bailey, Senior Research Scientist, Pacific Northwest National laboratory, and Dr. Benjamin Bond-Lamberty, Joint Global Change Research Institute in Maryland, visited the project sites to take preliminary samples for a cooperative study evaluating microbial functional processes across the hydrologic gradient within our study sites.

A Post-Doctoral Associate that was written into the project for 2.5 years has been hired at UCF. Dr. Scott Graham started on March 01, 2013 and is rapidly integrating into the research activities. He will be involved in Objectives 1-3 of the proposed work. Scott is interested in controls on terrestrial carbon storage. His research has focused on the role of temperature in regulating net ecosystem carbon balance and soil respiration. As well, he has investigated the impact of nitrogen fertilization and invasive species on carbon fluxes. He has worked primarily in grassland ecosystems, including New Zealand tussock grassland, tallgrass prairie and arctic tundra. Scott received his PhD from the University of Canterbury, completed his MS at the University of Illinois Chicago and has held several technical positions.

A new PhD graduate student in the Geosciences Department at FAU will be incorporated into this project as a Research Assistant by August of 2013. His main responsibilities will include static GPR surveys for underground biomass determination and time-lapse GPR surveys for investigating biogenic gas dynamics .

Up to four new graduate students (1 PhD, 3 MSc; pending acceptance of admission offer) in the Environmental Sciences Program at FAU will be incorporated into this project by August 2013 under Dr. Benscoter's supervision. These students will develop projects related to chamber and plant-level gas exchange, as well as quantification of plant and soil carbon stocks and the influence of fire on ecosystem carbon exchange. Additionally, an undergraduate student (Marina Lauck, FAU-Biological Sciences) will be testing a non-destructive technique for estimating aboveground biomass of sawgrass communities at the Blue Cypress Marsh (April 2013).

A Research Technician written into the project for 2 years at FAU has been recruited and is in the final stages of negotiation, with anticipated commencement in late April 2013. She will be responsible for assisting with the coordination and data collection of field campaigns as well as QA/QC and data management.

The project has been accepted for a North American Carbon program profile, http://www.nacarbon.org/cgi-bin/web/investigations/inv_pgp.pl?pgid=702

Appendix A

Carbon Dynamics and Sequestration Modeling Based on G'DAY Model

D. L. DeAngelis

This is a description of the carbon dynamics based on the G'DAY model of Comins and McMurtrie (1993) (see Figure 1). This is quite similar to a number of other models (e.g., CENTURY), but was simpler for me to modify this model, write my own source code and get it

running. This model will allow a detailed description of the allocation of nutrients between different plant parts (foliage, bole and branches, and roots). This fine scale division of nutrients corresponds reasonably close to how nutrients are measured in empirical studies. It will also allow the modeling and comparison of alternative allocation strategies of nutrients between the three main plant components. In addition, the G'DAY model allows for a realistic description of mineralization of the limiting nutrient. The G'DAY model was developed to follow the dynamics of carbon and nitrogen.

The dynamics of the carbon and nitrogen in the compartments is followed by means of differential equations for carbon and nitrogen in each compartment. The left hand sides of these equations represent the rate at which the amount of C or N in a compartment is changing, and the right-hand side represents the difference between fluxes going into and out of each compartment.

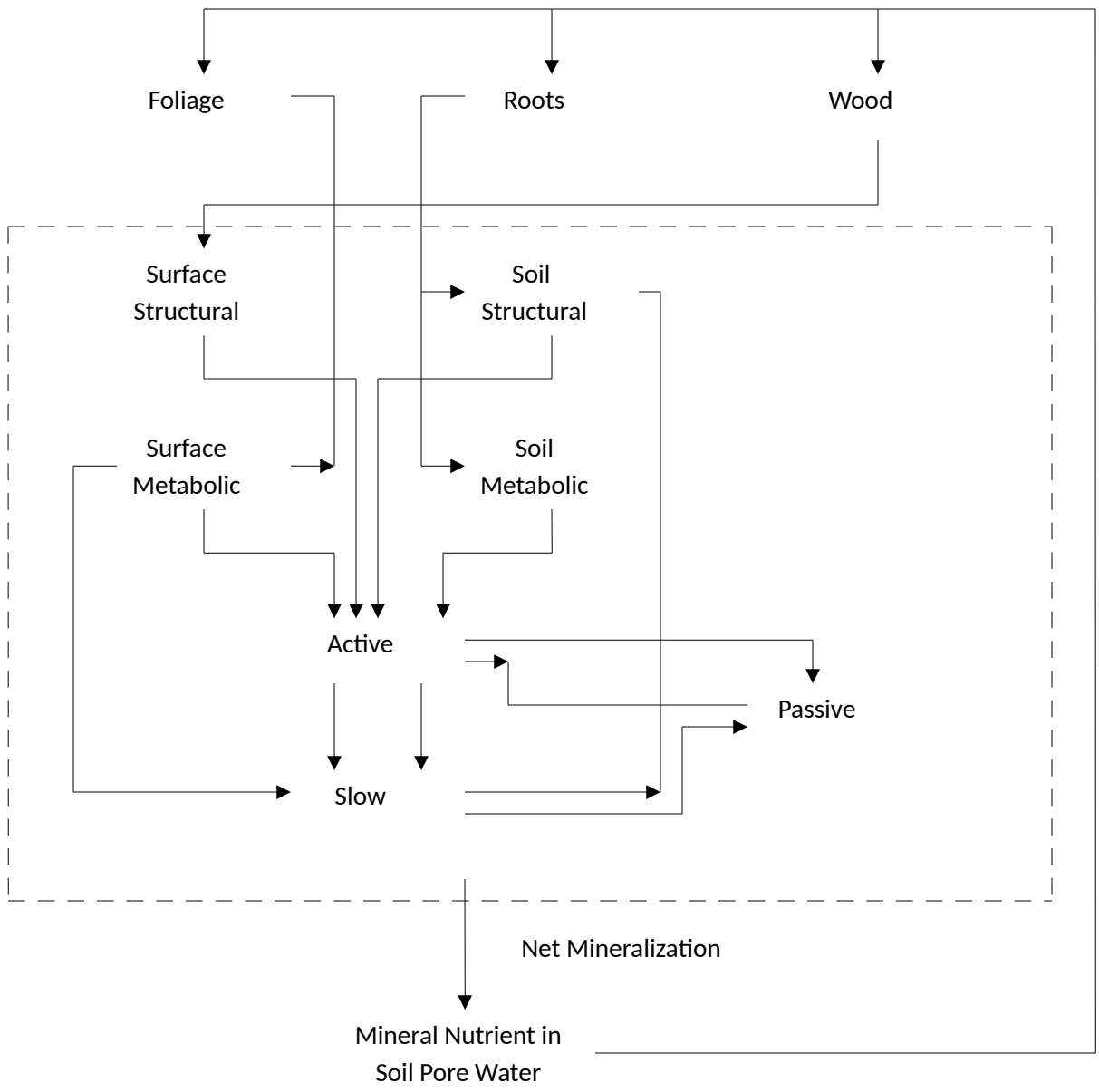

Figure 1.Schematic of nutrient flows and compartments in the G'DAY model. The net mineralization from the area enclosed in the dashed box is a result of decomposition phenomena of all litter and soil compartments. At times there is also some reverse flow of nutrients from the soil pore water to the two metabolic (microbial) compartments, surface and soil metabolic.

Basic Components of G'DAY Model

The carbon amounts in the compartments are denoted by *C* and the nitrogen amounts in the compartments are denoted by *N*. The following subscripts identify the compartments.

Tree Biomass Components

f	=	Foliage
w	=	Wood (in stem, branches, and large structural roots)
r	=	Coarse and fine roots

Litter Fractions

m	=	Surface metabolic litter
n	=	Soil metabolic litter
u	=	Surface structural litter
v	=	Soil structural litter

Soil Organic Matter Pools

a	=	Active
s	=	Slow
p	=	Passive

Mineral Pool

pore	=	Soil pore water

Both carbon and nitrogen pools are stored each of these compartments, except the mineral pool, which stores only nitrogen. These pools are dynamic, meaning that they can change through time. In mathematical terms, these pools are called variables.

Description of Changes Through Time of Each of the Pools

The rate of change of any pool (variable) is equal to the difference between the incoming and outgoing flows or fluxes. So we set the rate of change of a variable *X*, *dX/dt*, to the difference between the fluxes. The task in developing a model is identifying all of the fluxes.

A. Equations for plant carbon pools:

$$\frac{dC_f}{dt} = \eta_f G - \gamma_f C_f \quad \textbf{(1)}$$

$$\frac{dC_t}{dt} = \eta_r G - \gamma_r C_r \quad \textbf{(2)}$$

$$\frac{dC_w}{dt} = \eta_w G - \gamma_w C_w \quad \textbf{(3)}$$

where

C_f= foliage carbon pool (Mg ha^{-1})

C_r= root carbon pool (Mg ha^{-1})

C_w = wood carbon pool (Mg ha^{-1})

η_f = allocation fraction of carbon to foliage

η_r = allocation fraction of carbon to root

η_w = allocation fraction of carbon to wood

γ_f = senescence rate of foliage (yr^{-1})

γ_r = senescence rate of root (yr^{-1})

γ_w = senescence rate of wood (yr^{-1})

G= net carbon production, or growth per unit time (Mg ha^{-1} yr^{-1})

$= \varphi_0 \varepsilon_0 \omega R([CO_2]) I(F) E(v_f)$

where

φ_0 = incident photosynthetically active radiation (PAR) (GJ m^{-2} yr^{-1})

ε_0= potential PAR utilization efficiency at current ambient CO_2 concentration (kg/GJ)

ω = carbon content of biomass (fractional weight)

$R([CO_2])$ = growth response to ambient CO_2

$$= \frac{1.632([CO_2] - 60.9)}{[CO_2] + 121.8}$$

Note $R([CO_2])$ = 1 if we insert $[CO_2] = 350$.

$I(F)$ = light interception factor

$= 1 - exp(-k\sigma F/\omega)$

where

k = light extinction coefficient

σ = Specific leaf area. This is similar to leaf area index (LAI), but is actually leaf biomass per unit area of ground (m^2 kg^{-1})

F = foliage carbon content per ground area (Mg ha^{-1})

Note that $\sigma F/\omega$ = LAI, except that it has units m^2/ha, which needs to be corrected to get m^2/m^2 or ha/ha.

More detailed explanation of *G*:

G = net carbon production, or growth per unit time (Mg ha^{-1} yr^{-1})

= $\varphi_0\varepsilon_0\omega R([CO_2])I(F)E(\nu_f)$

where

φ_0 = incident photosynthetically active radiation (PAR) (GJ m^{-2} yr^{-1})

ε_0= potential PAR utilization efficiency at current ambient CO_2 concentration (kg/GJ)

ω = carbon content of biomass (fractional weight)

Note that

$\varphi_0\varepsilon_0$= kg dry weight biomass produced m^{-2} yr^{-1}

Therefore

$\varphi_0\varepsilon_0\omega$ = kg carbon produced m^{-2} yr^{-1}

The function

$R([CO_2])$ = growth response to ambient CO_2

$$= \frac{1.632([CO_2] - 60.9)}{[CO_2] + 121.8}$$

just estimates the effect of different levels of ambient CO_2 in the atmosphere.

Next let's consider the Light Interception Factor:

$I(F) = 1 - exp(-k\sigma F/\omega)$

where

σ = specific leaf area, or the area of leaves per kg of foliar dry biomass

= 5 m^2/kg dry mass

ω = fraction of dry biomass that is carbon
= 0.45

k = radiation extinction coefficient, or the fractional decrease in light for every unit of leaf area index (LAI) passed through
= 0.5

Therefore, it must be that

F = foliar dry weight carbon/m^2
= C_f

This means that

LAI = $\sigma F/\omega$ m^2 /m^2

Nutrient limitation factor:

We have

$E(v_f)$ = rate-limiting effect of low nitrogen concentration

where

$E(v_f)$ = 1 if $v_f > v_0$

$E(v_f)$ = v_f/v_0 if $v_f < v_0$

v_f = N:C ratio in foliage

v_0= threshold N:C ratio, above which nitrogen does not limit primary production

This just means that nutrient is limiting below the N:C ratio of v_0.

B. Equations for plant nitrogen pools:

$$\frac{dN_f}{dt} = (U + \Re - \eta_w \nu_w G)[\frac{\eta_f}{\eta_f + \rho\eta_r}] - \gamma_f N_f \quad \textbf{(4)}$$

$$\frac{dN_r}{dt} = (U + \Re - \eta_w \nu_w G)[\frac{\rho\eta_r}{\eta_f + \rho\eta_r}] - \gamma_r N_r \quad \textbf{(5)}$$

$$\frac{dN_w}{dt} = \eta_w \nu_w G - \gamma_w \nu_w C_w \quad \textbf{(6)}$$

where

N_f = foliage nitrogen pool (Mg ha^{-1})

N_r = root nitrogen pool (Mg ha^{-1})

N_w = wood nitrogen pool (Mg ha^{-1})

ρ= ratio of root N:V to foliage N:C ratio (assumed constant)

U = uptake rate of plant-available nitrogen (see below) (Mg ha^{-1} yr^{-1})

$\Re$ = nitrogenretranslocation rate (Mg ha^{-1} yr^{-1})

$$\Re = (1 - \lambda_f)\gamma_f N_f + (1 - \lambda_r)\gamma_r N_r$$

where

ν_f = N:C ratio for foliage

ν_r = N:C ratio for roots

ν_w = N:C ratio for wood

λ_f = ratio of litter N:C to live leaf N:C

λ_r = ratio of litter N:C to live root N:C

γ_w = senescence rate for foliage (yr^{-1})

γ_r = senescence rate for root (yr^{-1})

γ_w = senescence rate for wood (yr^{-1})

Note: as the leaf senesces, N is pulled back from leaf if the ratio of litter N:C to live leaf N:C, λ_f, is not equal to 1. The same happens in the roots if N:C to live leaf N:C, λ_r, is not equal to 1.

<u>Production of plant-available nitrogen, *U*</u>

$$U = (1 - \xi)[\aleph_M + \aleph_A + \aleph_F]$$

where

$\aleph_M$ = rate of nitrogen mineralization (excess of nitrogen inflows over outflows).

We will discuss this later. It is complicated. (Mg ha^{-1} yr^{-1})

$\aleph_A$ = rate of atmospheric nitrogen deposition (Mg ha^{-1} yr^{-1})

$\aleph_F$ = rate of nitrogen fixation (Mg ha^{-1} yr^{-1})

ξ = nitrogen emission fraction (N emitted as gases)

How do we interpret these three equations for the nitrogen pools in the plant?

The first thing to realize is that the ratio of N:C in wood is fixed. Therefore, the rate at which N is taken up by the wood compartment, $\eta_w \nu_w G$, is just ν_w (or the fixed N:C ratio in wood) multiplied by the rate of carbon increase in wood, $\eta_w G$.

Now we must interpret the inputs of N to foliage and roots. That is more complex, because the ratio of N:C in these compartments is not fixed, but can vary, although the ratio of these two ratios, (root N:C) : (foliage N:C) is fixed at ρ. What that means is that although neither N:C ratio is absolutely fixed, the two are fixed in relation to each other. To explain the input terms to foliage and roots, we note, first of all, there are two sources of N for the foliage and roots; the input of new N from outside, U, and the translocation of N from other parts of the plant (roots to foliage or vice versa), $\Re$. So we can imagine that the sum, $U + \Re$, is coming into the

combined roots and foliage (ignore the $-\eta_w \nu_w G$ terms for the moment). This is divided between the roots and foliage according to the ratios

$$\frac{\eta_f}{\eta_f + \rho\eta_r} \quad \text{and} \quad \frac{\rho\eta_r}{\eta_f + \rho\eta_r}$$

The first of these terms tells us the fraction of the input that goes to foliage, taking into account both the rate of carbon growth of foliage and the roots. If the ratio of N:C in foliage and roots were the same, then we would have $\rho = 1$. If the roots would have a higher N:C ratio than foliage (i.e., $\rho > 1$), then the fraction of N going to the roots would be greater than it would be if N were divided purely in terms of the carbon growth of these two compartments. Note that these two fractions sum to 1. Now, let's consider what the $-\eta_w \nu_w G$ terms mean. All these means is that a fixed amount, $-\eta_w \nu_w G$, is subtracted away from what comes into the plant and goes to the wood. It is included as negative terms in the amounts going into foliage and roots, because it subtracts a definite amount away from what these compartments can get. In other words, foliage and roots share whatever is left over after a fixed portion has been taken out for wood.

Now we should consider where the uptake, U, comes from.

$$U = (1 - \xi)[\aleph_M + \aleph_A + \aleph_F],$$

which combines the rates of mineralization (we will describe how to calculate this later), atmospheric deposition, and N fixation. A fraction, ξ, of these is subtracted out as emissions to the atmosphere.

Now we need to describe what the translocation means;

$$\Re = (1 - \lambda_f)\gamma_f N_f + (1 - \lambda_r)\gamma_r N_r$$

What this means is that, as leaves and roots senesce (die and drop off) at rates $\gamma_f N_f$ and $\gamma_r N_r$, respectively, some fractions $(1 - \lambda_f)$ and $(1 - \lambda_r)$, respectively, are taken back into the plant and redistributed proportionally to foliage and roots.

Finally, the losses from these compartments are proportional to the senescence (or death) of foliage, roots, and wood. Since the N:C ratios are variable in foliage and roots, the loss rates from those compartments have to be written as $\gamma_f N_f$ and $\gamma_r N_r$, respectively, whereas the loss from wood is written simply proportional to carbon loss, $\gamma_w v_w C_w$.

C. Equations for litter carbon pools:

Now we consider the changes in carbon in the four components of litter;
surface structural litter (C_u), surface metabolic litter (C_m), soil structural litter (C_v), and soil metabolic litter (C_n):

$$\frac{dC_u}{dt} = p_{uf}\gamma_f C_f + \gamma_w C_w - d_1' C_u \tag{7}$$

$$\frac{dC_m}{dt} = p_{mf}\gamma_f C_f - d_2' C_m \tag{8}$$

$$\frac{dC_v}{dt} = p_{vr}\gamma_r C_r - d_3' C_v \tag{9}$$

$$\frac{dC_n}{dt} = p_{nr}\gamma_r C_r - d_4' C_n \quad (10)$$

where

C_u= carbon in surface structural litter fraction (Mg ha^{-1})

C_m= carbon in surface metabolic litter fraction (Mg ha^{-1})

C_v = carbon in soil structural fraction (Mg ha^{-1})

C_n = carbon in soil metabolic fraction (Mg ha^{-1})

p_{ij} = fraction of carbon flow from soil pool j partitioned into pool i

d_i' = decomposition rates(yr^{-1})

There are specific expressions for the fractional allocations and decomposition rates

$p_{mf} = 1 - p_{uf} = 0.85 - 0.018\, L_{fl}/(\omega\lambda_f \nu_f)$

$p_{nr} = 1 - p_{vr} = 0.85 - 0.018\, L_{rl}/(\omega\lambda_r \nu_r)$

$d_1' = 0.076 exp(-3\, L_{fl})\, A(T_{soil})$

$d_2' = 0.29\, A(T_{soil})$

$d_3' = 0.094 \exp(-3\, L_{rl}) A(T_{soil})$

$d_4' = 0.35 A(T_{soil})$

$d_5' = 0.14(1 - 0.75T) A(T_{soil})$

where

L_{fl}= lignin to biomass ratio in leaf = 0.2

L_{rl} = lignin to biomass ration in root = 0.16

ω = 0.45

$A(T_{soil})$ = soil-temperature activity factor

= $0.0326 + 0.00351(T_{soil})^{1.652} – (T_{soil}/41.748)^{7.19}$

T_{soil} = average soil temperature

Assume

T_{soil} = 25.0

D. Equations for soil organic matter carbon pools:

$$\frac{dC_a}{dt} = p_{au}d_1{}'C_u + p_{am}d_2{}'C_m + p_{av}d_3{}'C_v + p_{an}d_4{}'C_n + p_{as}d_6{}'C_s + p_{ap}d_7{}'C_p - d_5{}'C_a \quad (11)$$

$$\frac{dC_s}{dt} = p_{su}d_1{}'C_u + p_{sv}d_3{}'C_v + p_{sa}d_5{}'C_a - d_6{}'C_s \quad (12)$$

(13)

$$\frac{dC_p}{dt} = p_{pa} d_5' C_a + p_{ps} d_6' C_s - d_7' C_p$$

where

C_a= carbon in active soil organic pool (Mg ha^{-1})

C_s = carbon in slow soil organic pool (Mg ha^{-1})

C_p = carbon in passive soil organic pool (Mg ha^{-1})

$p_{au} = 0.55(1 - L_{fl})$

$p_{su} = 0.7 L_{fl}$

$p_{av} = 0.45(1 - L_{fl})$

$p_{sv} = 0.7 L_{fl}$

$p_{am} = 0.45$

$p_{an} = 0.45$

$p_{sa} = 0.996 - [0.85 - 0.68\ T]$

$p_{pa} = 0.004$

$p_{as} = 0.42$

$p_{ps} = 0.03$

$p_{ap} = 0.45$

$d_6' = 0.0038\ A(T_{soil})$

$d_7' = 0.00013\ A(T_{soil})$

T =soil texture parameter = 0.5

L_{fl}= lignin to biomass ratio in leaf = 0.2

L_{rl} = lignin to biomass ration in root = 0.16

E. Equations for litter nitrogen pools:

$$\frac{dN_u}{dt} = \nu_u \Im_u - d_1' N_u \quad (14)$$

$$\frac{dN_m}{dt} = \aleph_{mf} + \aleph_{mw} - d_2' N_m \quad (15)$$

$$\frac{dN_v}{dt} = \nu_r \Im_v - d_3' N_v \quad (16)$$

$$\frac{dN_n}{dt} = \aleph_{nr} - d_4' N_n \quad (17)$$

N_u= nitrogen in surface structural litter fraction (Mg ha^{-1})

N_m= nitrogen in surface metabolic litter fraction (Mg ha^{-1})

N_v = nitrogen in soil structural fraction (Mg ha^{-1})

N_n = nitrogen in soil metabolic fraction (Mg ha^{-1})

$\Im_u, \Im_v$ = total carbon inflow to structural pools

$$\Im_u = p_{uf} \gamma_f C_f + \gamma_w C_w$$

$$\Im_v = p_{vr} \gamma_r C_r$$

$\aleph_{mf}$ = flow of nitrogen from foliage to surface metabolic fraction of litter

$\aleph_{mw}$ = flow of nitrogen from wood to surface metabolic fraction of litter

$\aleph_{nr}$ = flow of nitrogen from roots to soil metabolic fraction

What the above equations mean will require some explanation. We start with the fact there are flows from the foliage, wood, and roots going to the litter. We see above that the total carbon flows to the structural parts of the surface and soil litter are, respectively,

$$\Im_u = p_{uf}\gamma_f C_f + \gamma_w C_w$$

$$\Im_v = p_{vr}\gamma_r C_r \quad ,$$

where the flux to the surface structural litter comes from both foliage and wood and the flux to the soil structural litter comes from dead roots. Comins and McMurtrie make the assumption that the structural parts of the litter have N:C ratios of 1/150. That means that enough N must go to the structural components to match the C flow. So we must have

$$\nu_u \Im_u = \nu_u (p_{uf}\gamma_f C_f + \gamma_w C_w)$$

$$\nu_r \Im_v = \nu_r (p_{vr}\gamma_r C_r)$$

amount of N going to those structural components of the litter, N_u and N_v, where ν_u = 1/150 and ν_v = 1/150 multiplied by the fluxes of carbon from aboveground and belowground, respectively, to those structural components. It is an absolute, fixed, requirement that this much N goes to the two structural litter components. The flows of N out of these compartments are simply the decomposition rates multiplied by the standing stocks, $d_2'N_m$, and $d_4'N_n$. So the equations for the two structural components are pretty easy.

It is important at this point to recall the total amounts of N that are coming into the litter from the foliage and wood, and from the roots. What is coming to the surface (from foliage and wood) is

$$\gamma_f \lambda_f N_f + \gamma_w N_w \quad ,$$

while what is coming to the soil (from roots) is

$$\gamma_n \lambda_r N_r$$

Recall that the λ_f and λ_r , which are both less than 1, represent the fact that some nutrient has been retranslocated back to the tree foliage and roots. We have noted about that some amount of this nitrogen flux in the litter goes straight into the structural components. That part is a fixed ratio of the carbon that goes to the structural components. It cannot alter. But what about the surface

and soil metabolic components? The metabolic components are the microbes. We know they tend to be fussy. They like to have N:C ratios within a narrow range of values.

Let's now consider the fluxes of N to the metabolic components, N_m and N_n. This is not so easy as the structural components. It turns out that we must keep track of the N:C ratios in new litter coming in from the trees. The N:C ratio coming into surface metabolic litter is the ratio of total nitrogen from foliage and wood, minus that which is needed for the structural litter, to the carbon that goes to the metabolic component:

$$\gamma_f \lambda_f N_f + \gamma_w N_w - \nu_u \Im_u \; : \; p_{mf} \gamma_f C_f$$

Similarly, the N:C ratio coming into soil metabolic litter is:

$$\gamma_r \lambda_r N_r - \nu_v \Im_v \; : \; p_{vr} \gamma_r C_r$$

Depending on what these ratios are, different things can happen, and the inputs to the metabolic components, $\aleph_{mf} + \aleph_{mw}$ and $\aleph_{nr}$, respectively, can be quite different.

In fact, three things can happen with respect to these components.

Case 1. It is assumed in this model, that the microbes are happy if the N:C ratios they receive are in the narrow range: $1/25 < \text{N:C} < 1/10$. If the ratios are within this range, then the metabolic components simply take up the N that is left over after the N that must go to structural components is subtracted out. In that case, the uptake rates are just what is called the unconstrained form:

(flux to N_m)

$$\aleph_{mf} + \aleph_{mw} = \gamma_f \lambda_f N_f + \gamma_w N_w - \nu_u \Im_u$$

(flux to N_n)

$$\aleph_{nr} = \gamma_r \lambda_r N_r - \nu_v \Im_v$$

The total flux of N to the surface structural and metabolic compartments is equal to the sum of the rates of senescence of foliage and wood; $\gamma_f \lambda_f N_f + \gamma_w N_w$. Note that we have stuck a λ_f into the flux from foliage, because it is minus the retranslocated fraction $1 - \lambda_f$. A fixed amount of this

has to go to the surface structural component $\nu_\nu \Im_\nu$. So that leaves what we see in the first of

the above equations. The second equation follows from similar arguments for the soil structural and metabolic fractions, coming from the roots.

The important thing in this case is that exactly the same amount of N that falls as litter (both from foliage and wood on the surface and from roots underground) is taken into the four litter compartments. There is no excess or deficit of flux of N involved in the above case, where the ratios $\gamma_f \lambda_f N_f + \gamma_w N_w - \nu_u \Im_u$: $p_{mf} \gamma_f C_f$ and

$\gamma_n \lambda_r N_r - \nu_\nu \Im_\nu$: $p_{\nu r} \gamma_r C_r$ may lie in between 1/25 and 1/10. All the nitrogen that falls goes into

the structural and metabolic components and the metabolic component (microbes) do not need to take any nitrogen up from the soil pore water.

Now we must consider the cases in which both or either $\gamma_f \lambda_f N_f + \gamma_w N_w - \nu_u \Im_u$: $p_{mf} \gamma_f C_f$

and $\gamma_n \lambda_r N_r - \nu_\nu \Im_\nu$: $p_{\nu r} \gamma_r C_r$ ratios are higher than 1/10 or lower than 1/25. (Keep in mind that

the surface and underground situations are independent of each other and could differ in their ratios.)

Case 2. Both or either of the ratios of incoming litter N : C are very low (< 1/25). We can guess that in this case the metabolic component or components need N badly and will try to keep the N:C ratio in their bodies from going any lower than 1/25. We can guess that a metabolic component will have a net uptake of N from the mineral nitrogen pool (immobilization). In this situation the input of N is called a ‘constrained form’, as described now.

In this ‘constrained’ case we have

$$\aleph_{mf} + \aleph_{mw} = \nu_m p_{mf} \gamma_f C_f$$

$$\aleph_{nr} = \nu_n p_{nr} \gamma_r C_r$$

So, for example, if $\gamma_f \lambda_f N_f + \gamma_w N_w - \nu_u \Im_u$: $p_{mf} \gamma_f C_f$ < 1/25 then

$\aleph_{mf} + \aleph_{mw}$ takes on the form shown above and v_m takes on the value 1/25, because the microbes must maintain at least that ratio in their intake. Similarly if $\gamma_n \lambda_r N_r - v_v \Im_v : p_{vr} \gamma_r C_r$ < 1/25 then $\aleph_{nr}$ takes on the above form and $v_n$takes on the value 1/25, again because the microbes need at least that high a ratio of N to C. What this means is that if the N:C ratio in incoming litter to the metabolic components is low (< 1/25), then the metabolic component will take up N at a rate of one mole for every 25 moles of C. It will have to do this by taking up N from the surrounding soil pore water.

In that case the uptake of N by the litter components does not equal the amount of N input from litterfall. There will be net immobilization of N in the soil pore water (discussed later).

Case 3. Both or either of the ratios of incoming litter N to C may be very high (> 1/10) such that this compartment has a net release to the mineral nitrogen pool (mineralization).
This is again a constrained form. In this case we have

$$\aleph_{mf} + \aleph_{mw} = v_m p_{mf} \gamma_f C_f$$

$$\aleph_{nr} = v_n p_{nr} \gamma_r C_r$$

So for example, if $\gamma_f \lambda_f N_f + \gamma_w N_w - v_u \Im_u : p_{mf} \gamma_f C_f$ > 1/10 then $\aleph_{mf} + \aleph_{mw}$ takes on the form shown above and v_m takes on the value 1/10, because the microbes do not want to take up any more N than that ratio. Similarly if $\gamma_n \lambda_r N_r - v_v \Im_v : p_{vr} \gamma_r C_r$ > 1/10 then $\aleph_{nr}$ takes on the above form and v_n takes on the value 1/10, again because the microbes do not need all of that nitrogen. What this means is that if the N:C ratio in incoming litter to the metabolic components is high (> 1/10), then the metabolic component will take up N at a rate of one mole for every 10 moles of C. It will have to do this by giving up N to the surrounding soil pore water.

In that case the uptake of N by the litter components does not equal the amount of N input from litterfall. There will be net mineralization of N to the soil pore water (discussed later).

So, for purposes of the computer model, we must keep track of the

$$\gamma_f \lambda_f N_f + \gamma_w N_w - v_u \Im_u \quad : \quad p_{mf} \gamma_f C_f$$

$$\gamma_r \lambda_r N_r - v_v \Im_v \quad : \quad p_{vr} \gamma_r C_r$$

ratios and determine the forms of , and , depending on what those ratios are.
$\aleph_{mf} + \aleph_{mw}$ $\aleph_{nr}$

We will calculate later exactly how these considerations affect the net mineralization vs. immobilization.

The parameter values are

$v_u = v_v = 1/150$

$v_a = 1/15$

$v_s = 1/20$

$v_p = 1/10$

$v_m = 1/10$ or $1/25$

$v_n = 1/10$ or $1/25$

Below, we show diagrams (Figures 2 and 3) of nitrogen and carbon from surface litter (wood and foliage) to the surface structural and metabolic components and show how this leads to each of the three cases.

Nitrogen Flows to Surface Litter, both Structural and Metabolic

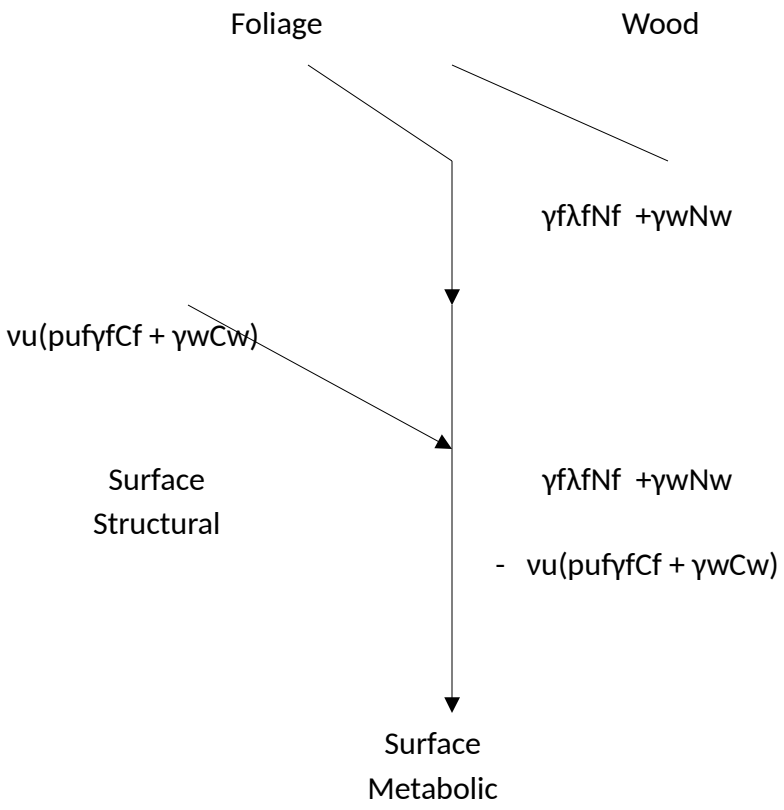

Figure 2. Schematic of fluxes of how fluxes of nitrogen from foliage and wood are divided among surface structural and surface metabolic compartments.

Carbon Flows to Surface Litter, both Structural and Metabolic

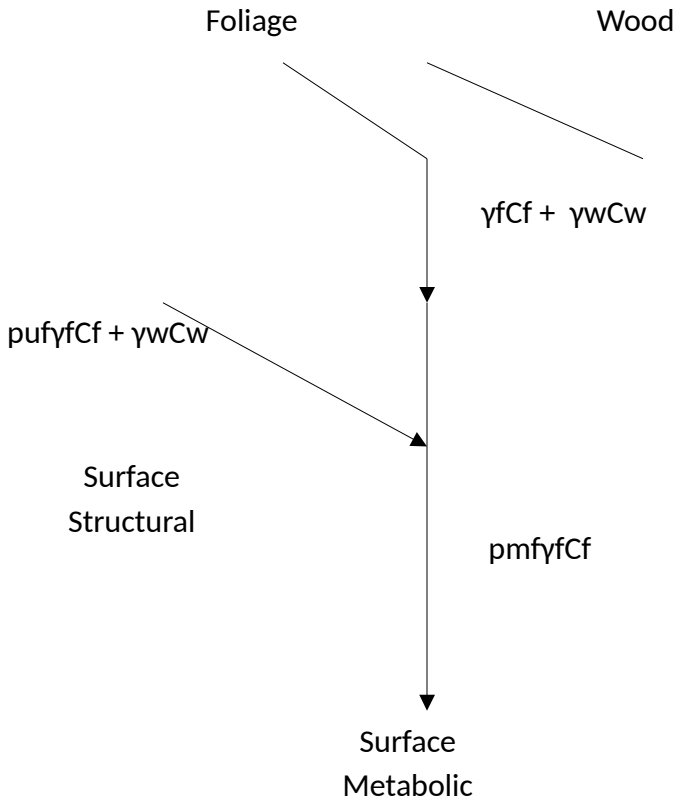

Figure 3. Schematic of fluxes of how fluxes of carbon from foliage and wood are divided among surface structural and surface metabolic compartments.

If litter N:C ratio going to surface metabolic is

$1/25 < \gamma_f \lambda_f N_f + \gamma_w N_w - v_u(p_{uf}\gamma_f C_f + \gamma_w C_w) : p_{mf}\gamma_f C_f < 1/10$, **then**

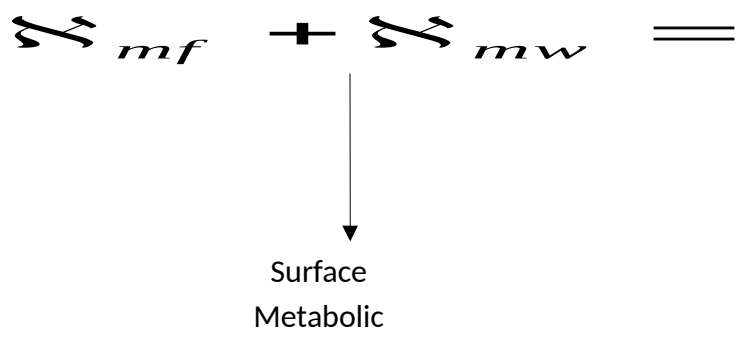

If litter N:C ratio to metabolic is

$\gamma_f \lambda_f N_f + \gamma_w N_w - v_u(p_{uf}\gamma_f C_f + \gamma_w C_w)) : p_{mf}\gamma_f C_f < 1/25$, **then**

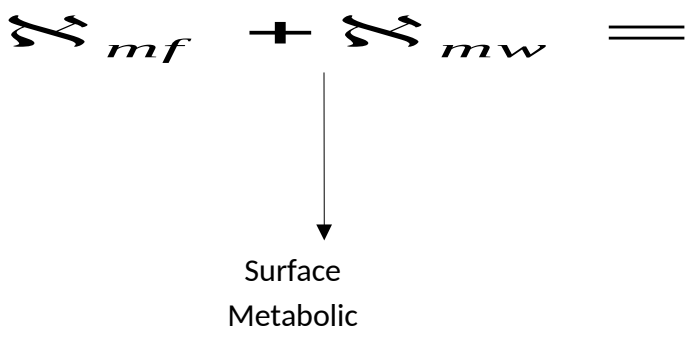

In this case, the microbes (surface metabolic compartment) needs to take up some of their nitrogen from the soil pore water to make up for the fact that the nitrogen from litter

$\gamma_f \lambda_f N_f + \gamma_w N_w - v_u(p_{uf}\gamma_f C_f + \gamma_w C_w)) < (1/25) p_{mf}\gamma_f C_f$

is not sufficient to balance the carbon going into microbial biomass. Net immobilization occurs.
If litter N:C ratio to metabolic is

1/10 $< \gamma_f \lambda_f N_f + \gamma_w N_w - v_u(p_{uf}\gamma_f C_f + \gamma_w C_w)) : p_{mf}\gamma_f C_f$, **then**

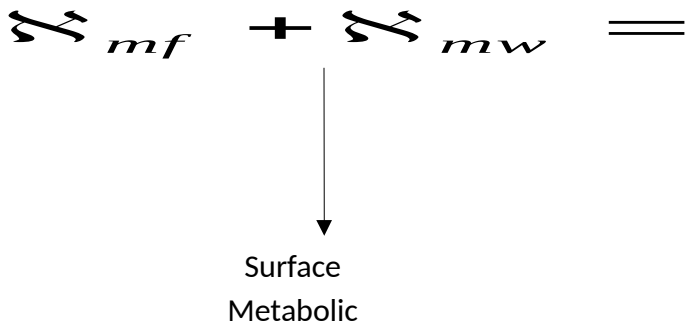

In this case, the microbes (surface metabolic compartment) can release nitrogen into the soil pore water, because the nitrogen from litter

$\gamma_f \lambda_f N_f + \gamma_w N_w - v_u(p_{uf}\gamma_f C_f + \gamma_w C_w)) > (1/10) p_{mf}\gamma_f C_f$

is more than sufficient to balance the carbon going into microbial biomass. So net mineralization occurs.

We can see that the criteria for mineralization are a bit more complex than they are in Parnas's model and in the EXPLORE model. In the EXPLORE model, mineralization only takes place when the N:C ratio in soil is greater than 1/20. Otherwise, immobilization (of the ½ unit of N that comes from outside each year) occurs. There is also a similar simple threshold relationship in Parnas's model. However, in G'DAY, things are a bit more complex. Net mineralization occurs when the N:C ratio in litter to the metabolic component is greater than 1/10. Net immobilization occurs when the N:C ratio in the litter to the metabolic component is less than 1/25. Between those thresholds, all that happens is that the ratio of N:C in the metabolic component (microbes) changes. So, by inclusion of a microbe component, G'DAY has some behaviors that we don't get in Parnas's model or the EXPLORE model.

F. Equations for soil organic matter nitrogen pools:

$$\frac{dN_a}{dt} = \nu_a \Im_a - d_5' N_a \quad (18)$$

$$\frac{dN_s}{dt} = \nu_s \Im_s - d_6' N_s \quad (19)$$

$$\frac{dN_p}{dt} = \nu_p \Im_p - d_7' N_p \quad (20)$$

N_a= nitrogen in active soil organic pool (Mg ha^{-1})

N_s = nitrogen in slow soil organic pool (Mg ha^{-1})

N_p = nitrogen in passive soil organic pool (Mg ha^{-1})

$\Im_a$ = flow of nitrogen to active soil fraction

$\Im_s$ = flow of nitrogen to slow soil fraction

$\Im_p$ = flow of nitrogen to passive soil fraction

where

$$\Im_a = p_{au} d_1' C_u + p_{am} d_2' C_m + p_{av} d_3' C_v + p_{an} d_4' C_n + p_{as} d_6' C_s + p_{ap} d_7' C_p$$

$$\Im_s = p_{su} d_1' C_u + p_{sv} d_3' C_v + p_{sa} d_5' C_a$$

$$\Im_p = p_{pa} d_5' C_a + p_{ps} d_6' C_s$$

Mineralization

Now we are in a position to calculate the mineralization, $\aleph_M$, that was defined way back in

"Section B: Equations for plant nitrogen pools".

Nitrogen mineralization rate is given by the excess of nitrogen outflows from all the compartments over the inflows to compartments. The outflows and inflows will not match. If the outflows exceed the inflows then there will be net increase in soil pore water (mineralization).

$$\aleph_M = \begin{array}{l} \gamma_f \lambda_f N_f + \gamma_r \lambda_r N_r + \gamma_w N_w + d_1' N_u + d_2' N_m + d_3' N_v + d_4' N_a + d_5' N_a \\ d_6' N_s + d_7' N_p - \\ \qquad v_u \Im_u - \aleph_{mf} - \aleph_{mw} - v_v \Im_v - \aleph_{nr} - v_a \Im_a - v_s \Im_s - v_p \Im_p \end{array} \quad (21)$$

Terms 1, 2, and 3 represent the outflow of N from foliage, roots, and wood to litter.

Terms 4, 5, 6, 7, 8, 9, and 10 represent the outflows of N from decomposition of surface structural, surface metabolic, soil structural, soil metabolic, soil active, soil slow, and soil passive compartments.

Terms 11, 12 + 13, 14, and 15 represent the inflows, or uptakes of N by surface structural, surface metabolic, soil structural, and soil metabolic compartments.

Terms 16, 17, and 18 represent inflows or uptakes of N by soil active, soil slow, and soil passive compartments.

There are some interesting things about $\aleph_M$.

First, let us assume that the whole system is at steady state. That means that the left hand sides of all 20 equations are equal to zero. In that case, you can see, by looking at equations (14) through (20) that

$$\aleph_M = \gamma_f\lambda_f N_f + \gamma_r\lambda_r N_r + \gamma_w N_w \quad (22)$$

So, at steady state there will be net mineralization. There has to be in order for steady state to occur. The alternative would be for some compartments to continue to build up in nitrogen forever. The fact that at steady state there is a constant rate of mineralization that is equal to the nitrogen in litterfall is perfectly consistent with Parnas's model and with the EXPLORE model.

Of course, we are not always interested in steady state, so if we make a disturbance at some point, such as increasing litterfall, then there will be changes in the mineralization rate, and even net immobilization at times, just as in Parnas's model and the EXPLORE model. But, given enough time, mineralization rate will always return to (22).

Extension of G'DAY model to include soil pore water nutrient concentration

The G'DAY model assumes that mineralized nitrogen, along with external inputs (nitrogen fixation and atmospheric deposition) go directly into plant uptake.

We want to modify the model so that the mineralized nitrogen goes into a soil pore water pool, where it can either be (1) immobilized by microbes, (2) leached from the soil, or (3) be taken up by plants. Therefore, we add a new component, soil porewater nutrient, N_{pore}, which will have the equation

$$\frac{dN_{pore}}{dt} = \gamma_f\lambda_f N_f + \gamma_r\lambda_r N_r + \gamma_w N_w + d_1'N_u + d_2'N_m + d_3'N_v + d_4'N_a + d_5'N_a$$

$$d_6'N_s + d_7'N_p - v_u\Im_u - \aleph_{mf} - \aleph_{mw} - v_v\Im_v - \aleph_{nr} - v_a\Im_a - v_s\Im_s - v_p\Im_p$$

$$+ N_{input} - QN_{pore} - U_{plant}$$

The first 18 terms determine whether net mineralization or immobilization are occurring. Term 19 represents external input, Term 20 represents leaching due to the flow of water through the system, and Term 21 represents uptake by the plant (see Figure 2 below).

We are currently working on a more complex modification that will involve soil porewater nutrient in two soil layers.

Additional parameter values used in the original G'DAY model.

η_f= 0.3

η_r= 0.3

γ_f= 0.5 yr^{-1}

γ_r= 1.5 yr^{-1}

γ_w = 0.01 yr^{-1}

ρ= 0.7

λ_f= 1

λ_r= 1

ω= 0.45

L_{fl}= 0.2

L_{rl} = 0.16

T = 0.5

ξ= 0.05

$\aleph_A + \aleph_F$ = 0.01 Mg ha^{-1} yr^{-1}

φ_0 = 3 GJ m^{-2} yr^{-1}

ε_0 = 2.8 kg GJ^{-1} (dry mass)

v_0 =0.04

k = 0.5

σ= 5 m^2kg^{-1} (dry mass)

We have extended the model to include external inputs to and leaching from the soil nutrient pool (Figure 4 below).

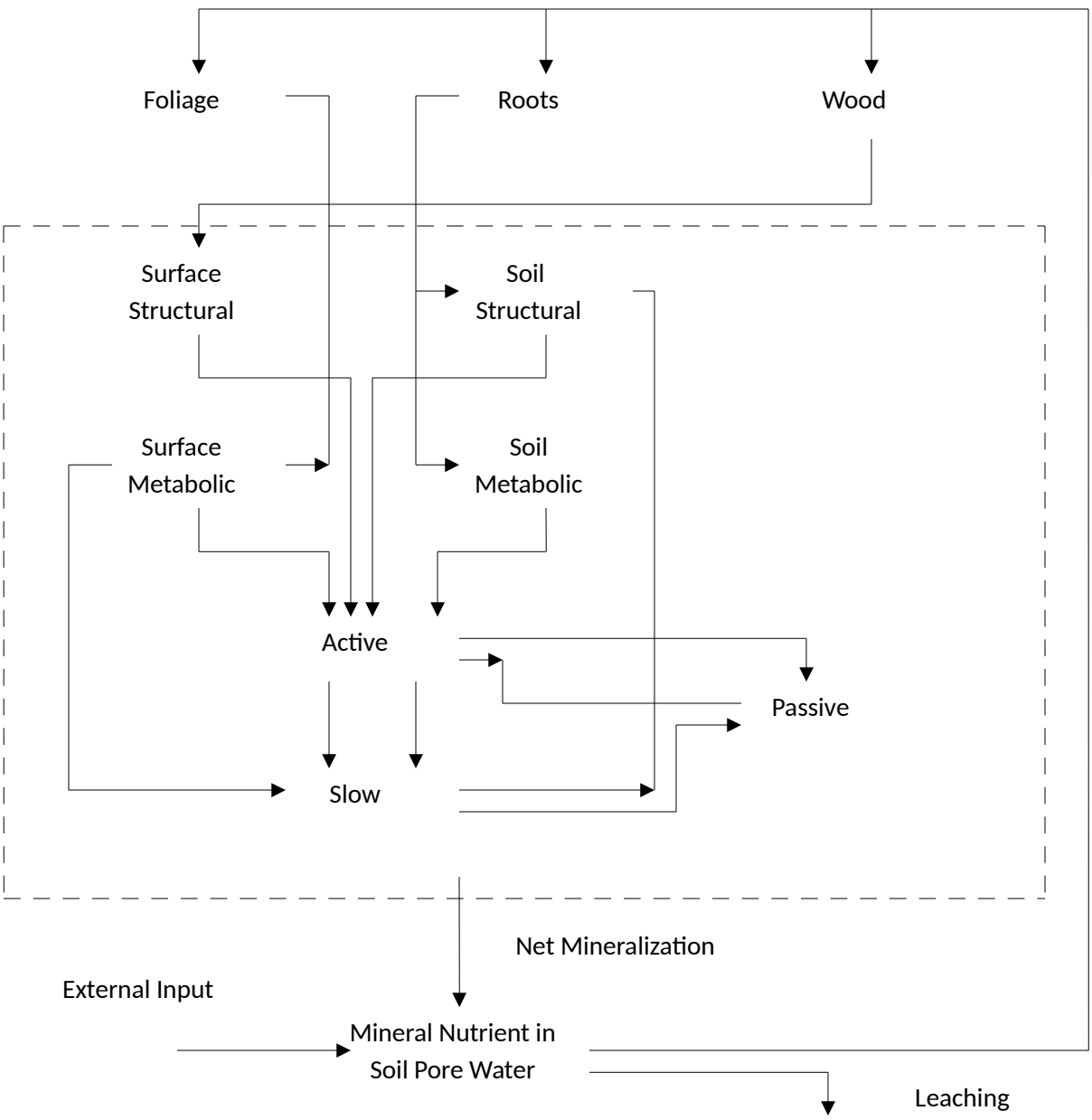

Figure 4.Schematic of nutrient flows and compartments in the modified G'DAY model. The net mineralization from the area enclosed in the dashed box is a result of decomposition phenomena of all litter and soil compartments. At times there is also some reverse flow of nutrients from the soil pore water to the two metabolic (microbial) compartments, surface and soil metabolic.

Some References

Comins, H. N., and McMurtrie, R. E.. 1993. Long-term response of nutrient-limited forests to CO_2 enrichment; equilibrium behavior of plant-soil models. Ecological Applications 3: page 666-681.

Parnas, H. 1975. Model for decomposition of organic material by microorganisms. Biology and Biochemistry 7:161-169.

Some Notes on the G'DAY Model

It appears that all of the variables in G'DAY are in Mg ha^{-1}. At least they should be treated that way.

We have to be careful to make sure that the inputs are expressed that way also. In particular, the input of nitrogen is set to

$$\aleph_A + \aleph_F = 1.0 \text{ g m}^{-2} \text{ yr}^{-1}$$

This should be multiplied by 0.01 to give the input rate in Mg ha^{-1} .

The growth rate, G, seems strange also. For example, it is stated that

ε_0 = 2.8 kg/GJ.

Actually,

ε_0 = 100 kg/GJ.

Then the maximum value of G would be

G = $\varphi_0 \varepsilon_0 \omega$ = 2.8 * 100 * 0.45 = 126. kg m^{-1}

However, when this is converted to Mg ha^{-1}, we get

G = 126. kg m^{-1} = 12.6 Mg ha^{-1}

So we should use this input in the model. However, I am using a somewhat lower value of about

G = 7.4 Mg ha^{-1}

as it seems to work better.

For possible inconsistencies of units, we should also take a look at

$I(F) = 1 - \exp(-\mathbf{k}\sigma F/\omega)$

Note that

k = extinction coefficient = 0.5

σ = 5 m^2 kg^{-1} (dry mass)

ω = carbon to biomass ratio = 0.45

F = foliage carbon (C_f) in Mg ha^{-1}